COQ11 deletion mitigates respiratory deficiency caused by mutations in the gene encoding the coenzyme Q chaperone protein Coq10

Received for publication, December 20, 2019, and in revised form, March 17, 2020 Published, Papers in Press, March 23, 2020, DOI 10.1074/jbc.RA119.012420

Michelle C. Bradley[‡], Krista Yang[‡], Lucía Fernández-del-Río[‡], Jennifer Ngo[‡§], Anita Ayer[¶‖], Hui S. Tsui[‡], Noelle Alexa Novales[‡], Roland Stocker[¶‖], Orian S. Shirihai[§], Mario H. Barros[**], and Catherine F. Clarke[‡1]

From the [‡]Department of Chemistry and Biochemistry, Molecular Biology Institute, UCLA, Los Angeles, California 90095-1569, the [§]Department of Molecular and Medical Pharmacology and Medicine, David Geffen School of Medicine, UCLA, Los Angeles, California 90095, the [¶]Vascular Biology Division, Victor Chang Cardiac Research Institute, Sydney, New South Wales 2010, Australia, the [‖]St. Vincent's Clinical School, University of New South Wales Medicine, Sydney, New South Wales 2050, Australia, and the [**]Departamento Microbiologia, Universidade de São Paulo, São Paulo 05508-900, Brazil

Edited by Dennis R. Voelker

Coenzyme Q (Q_n) is a vital lipid component of the electron transport chain that functions in cellular energy metabolism and as a membrane antioxidant. In the yeast *Saccharomyces cerevisiae*, *coq1–coq9* deletion mutants are respiratory-incompetent, sensitive to lipid peroxidation stress, and unable to synthesize Q_6. The yeast *coq10* deletion mutant is also respiratory-deficient and sensitive to lipid peroxidation, yet it continues to produce Q_6 at an impaired rate. Thus, Coq10 is required for the function of Q_6 in respiration and as an antioxidant and is believed to chaperone Q_6 from its site of synthesis to the respiratory complexes. In several fungi, Coq10 is encoded as a fusion polypeptide with Coq11, a recently identified protein of unknown function required for efficient Q_6 biosynthesis. Because "fused" proteins are often involved in similar biochemical pathways, here we examined the putative functional relationship between Coq10 and Coq11 in yeast. We used plate growth and Seahorse assays and LC-MS/MS analysis to show that *COQ11* deletion rescues respiratory deficiency, sensitivity to lipid peroxidation, and decreased Q_6 biosynthesis of the *coq10*Δ mutant. Additionally, immunoblotting indicated that yeast *coq11*Δ mutants accumulate increased amounts of certain Coq polypeptides and display a stabilized CoQ synthome. These effects suggest that Coq11 modulates Q_6 biosynthesis and that its absence increases mitochondrial Q_6 content in the *coq10*Δ*coq11*Δ double mutant. This augmented mitochondrial Q_6 content counteracts the respiratory deficiency and lipid peroxidation sensitivity phenotypes of the *coq10*Δ mutant. This study further clarifies the intricate connection between Q_6 biosynthesis, trafficking, and function in mitochondrial metabolism.

Coenzyme Q (ubiquinone or Q)[2] is a benzoquinone lipid that functions as an essential electron carrier within the electron transport chain (1). Because of its redox activities, Q is a versatile electron acceptor in biological pathways such as cellular respiration, oxidation of proline and sulfide, fatty acid β-oxidation, and pyrimidine biosynthesis (1–3). The reduced hydroquinone form of Q (ubiquinol or QH_2) also serves as an important chain-breaking antioxidant shown to alleviate lipid peroxidative damage in cellular membranes (4).

For proper functional localization, Q relies on its polyisoprenoid tail to remain anchored at the mid-plane of phospholipid bilayers. The number of isoprene units (n) that comprise the polyisoprenoid tail of Q_n depends on a species-specific polyprenyl diphosphate synthase (5), with Q_{10} representing the major isoform in humans (6). Patients unable to produce adequate levels of Q_{10} display a wide variety of health issues that stem from mitochondrial dysfunction across tissues (7). Attempts to ameliorate the consequences of primary Q_{10} deficiency by early Q_{10} supplementation have been partially successful in some cases (8); however, many patients fail to demonstrate full recovery, which is related to inefficient uptake of orally-supplied Q_{10}. Because of the striking homology between human *COQ* genes and those of *Saccharomyces cerevisiae* (7, 9), studies of Q_6 biosynthesis in *S. cerevisiae* may provide insight

This work was supported by National Science Foundation Grant MCB-1330803 (to C. F. C.), National Institutes of Health Grant T32 GM 007185 (to H. S. T. and M. C. B.) Ruth L. Kirschstein National Service (to M. C. B. and H. S. T.), the Whitcome Individual Predoctoral Fellowship (to M. C. B.), UCLA Summer Undergraduate Research Fellowship, Department of Chemistry and Biochemistry (to K. Y.), Fundação de Amparo a Pesquisa de São Paulo–FAPESP 2013/09482-8 and 2013/07937-8 (to M. H. B.), Gates Millennium Scholars Fellowship (to J. N.), and the Eugene V. Cota Robles Fellowship (to J. N.). The authors declare that they have no conflicts of interest with the contents of this article. The content is solely the responsibility of the authors and does not necessarily represent the official views of the National Institutes of Health.
This article contains Figs. S1–S3, Tables S1 and S2, and supporting Refs. 1–8.
[1] To whom correspondence should be addressed. Tel.: 310-825-0771; Fax: 310-206-5213; E-mail: cathy@chem.ucla.edu.

[2] The abbreviations used are: Q, ubiquinone; DMQ, demethoxy-Q; HHB, 3-hexaprenyl-4-hydroxybenzoic acid; Q_n, coenzyme Q_n (where n designates the number of isoprene units in the polyisoprenyl tail); QH_2, reduced coenzyme Q or ubiquinol; ORF, open reading frame; ER, endoplasmic reticulum; MIOREX complex, mitochondrial organization of gene expression complex; IMS, intermembrane space; OCR, oxygen consumption rate; FCCP, carbonyl cyanide *p*-trifluoromethoxyphenylhydrazone; PUFA, polyunsaturated fatty acid; qPCR, quantitative real-time PCR; ERMES, ER-mitochondrial encounter structure; START, steroidogenic acute regulatory protein–related lipid transfer; BisTris, 2-[bis(2-hydroxyethyl)amino]-2-(hydroxymethyl)propane-1,3-diol; SDR, short-chain dehydrogenase/reductase; 2D-BN/SDS-PAGE, two-dimensional blue native/SDS-PAGE; DOD, dropout dextrose; SD, synthetic dextrose; lc*COQ11*, low-copy *COQ11*; RET, reverse electron transport; P, pellet; S, supernatant.

into human Q_{10} biosynthesis, leading to the discovery of potential therapeutic targets.

In *S. cerevisiae*, at least 14 nuclear-encoded mitochondrial proteins (Coq1–Coq11, Yah1, Arh1, and Hfd1) drive Q_6 biosynthesis (7, 9). Many Coq polypeptides (Coq3–Coq9, and Coq11) are localized to the matrix side of the mitochondrial inner membrane, where they organize into a high-molecular-weight multisubunit complex known as the "CoQ synthome" (7, 9). Several lines of evidence suggest that correct assembly of the CoQ synthome is necessary for efficient Q_6 biosynthesis (9–12). In fact, deletion of certain *COQ* genes results in decreased levels of other Coq polypeptides and contributes to a destabilized CoQ synthome in these mutants (12, 13). Recently, a protein of unknown function encoded by the ORF *YLR290C* was identified to associate with the CoQ synthome, via proteomic analysis of tandem affinity-purified tagged Coq proteins (14). YLR290C copurified with Coq5, Coq7, and Coq9, in addition to Q_6 and late-stage Q_6-intermediates (14). Furthermore, the *ylr290c*Δ mutant exhibited impaired *de novo* Q_6 biosynthesis, despite preserving growth on a nonfermentable carbon source (14). Given its effects on Q_6 biosynthesis and involvement with the CoQ synthome, YLR290C was renamed Coq11 (14).

In several fungi, Coq11 and Coq10 have evolved as fusion proteins (14), suggesting that Coq11 may have a functional relationship with Coq10 (15). High-throughput genetic analyses found *COQ11* to correlate with both *COQ2* and *COQ10* (16). Whereas the *coq* mutants generally lack Q_6, the *coq10*Δ mutant is different because it produces near WT amounts of Q_6 in stationary phase and only has decreased *de novo* Q_6 biosynthesis in log phase (17, 18). Although Q_6 biosynthesis is only minimally decreased in the absence of *COQ10*, the *coq10*Δ mutant has decreased NADH and succinate oxidase activity and displayed sickly growth on respiratory medium (18). The *coq10*Δ mutant is sensitive to lipid peroxidation initiated by exogenously supplemented polyunsaturated fatty acids (PUFAs), indicating that the Coq10 polypeptide is also required for antioxidant protection by Q_6 (17, 19).

The NMR structure of a Coq10 ortholog in *Caulobacter crescentus* was shown to possess a steroidogenic acute regulatory protein–related lipid transfer (START) domain (20) that can directly bind Q and late-stage Q-intermediates (17). Purified Coq10 from either *S. cerevisiae* or *Schizosaccharomyces pombe* eluted with the respective species' Q isoform (18, 21). This observation has prompted speculation that Coq10 acts as a Q_6 chaperone protein required for delivery of Q_6 from its synthesis site to sites where Q_6 functions as an antioxidant and to the respiratory complexes, thereby bridging efficient *de novo* Q_6 biosynthesis with respiration (17). Recent studies have shown a spatial compartmentalization of the mitochondrial inner membrane with the identification of different sites, such as the inner boundary membrane, the cristae membrane, and the ER-mitochondrial contact sites (22–25). Thus, for optimal respiratory competence, newly-synthesized Q_6 must move from its site of synthesis (*i.e.* the ER-mitochondrial contact sites (23, 24)) to the cristae membrane where the respiratory complexes are concentrated (22). The presence of Coq10–Coq11 fusions in fungal species indicates that Coq11 may have a functional association with the Coq10 chaperone to facilitate or regulate Q_6 transport for respiration in yeast.

In this work, the functional relationship between Coq10 and Coq11 was investigated using a series of single- and double-knockout mutants. Deletion of *COQ11* alleviated the *coq10*Δ respiratory defect, increased Coq polypeptides and CoQ synthome stability, and partially rescued Q_6 production. Based on this evidence, we propose a novel function for Coq11 as a negative modulator of Q_6 biosynthesis in the mitochondria.

Results

Coq10 and Coq11 reside in similar compartments within the mitochondria

Previous phylogenetic analyses of numerous fungi revealed that Coq11-like proteins are fused to Coq10 (14). Protein fusions often indicate a functional relationship between corresponding homologs in other organisms, such as direct protein–protein interaction or operation within the same biological pathway (15). Although Coq10 and Coq11 are not physically fused in yeast (Fig. 1*A*), we sought to investigate whether there is a functional link between the two proteins. Because protein localization is often associated with function, we first performed mitochondrial fractionation to localize both Coq10 and Coq11. Coq10 has been localized previously (18), but fractionation was re-performed here in the context of Coq11.

S. cerevisiae mitochondria were fractionated as described under "Experimental procedures." Purified mitochondria were incubated in hypotonic buffer to disrupt the outer membrane and release soluble components of the intermembrane space (IMS). The inner membrane was kept intact following hypotonic buffer treatment, protecting inner membrane and matrix proteins. Analysis of the fractions via immunoblot suggested that both Coq10 and Coq11 remained associated with the mitoplast fraction as opposed to colocalizing with the IMS marker cytochrome b_2. Mitoplasts were further fractionated after sonication to separate soluble matrix components (supernatant, S) from membrane components (pellet, P). The soluble matrix marker Hsp60 was partially released into the supernatant by sonication as demonstrated in earlier work (26). Although Coq11 remained associated with the membrane fraction, Coq10 was partially dissociated in a similar manner to Hsp60 (Fig. 1*B*). Previous Coq10 colocalization following sonication demonstrated that Coq10 was solely associated with the membrane fraction (18). The detection of Coq10 in the supernatant shown in Fig. 1*B* may be due to increased sensitivity of the polyclonal antisera used in this study.

Alternatively, mitoplasts were subjected to alkaline carbonate extraction to separate peripheral membrane components (supernatant, S) from integral membrane and matrix components (pellet, P) (27). Coq10 and Coq11 were released into the supernatant following alkaline treatment (Fig. 1*B*), matching the peripheral inner membrane marker Atp2 (28). There was no colocalization with the pellet fraction, marked by the integral membrane protein Cyt_1 (29). These results indicate that Coq10 and Coq11 are both peripheral inner membrane proteins, and Coq10 has additional localization to the matrix. The localization of Coq10 to the inner membrane is consistent with

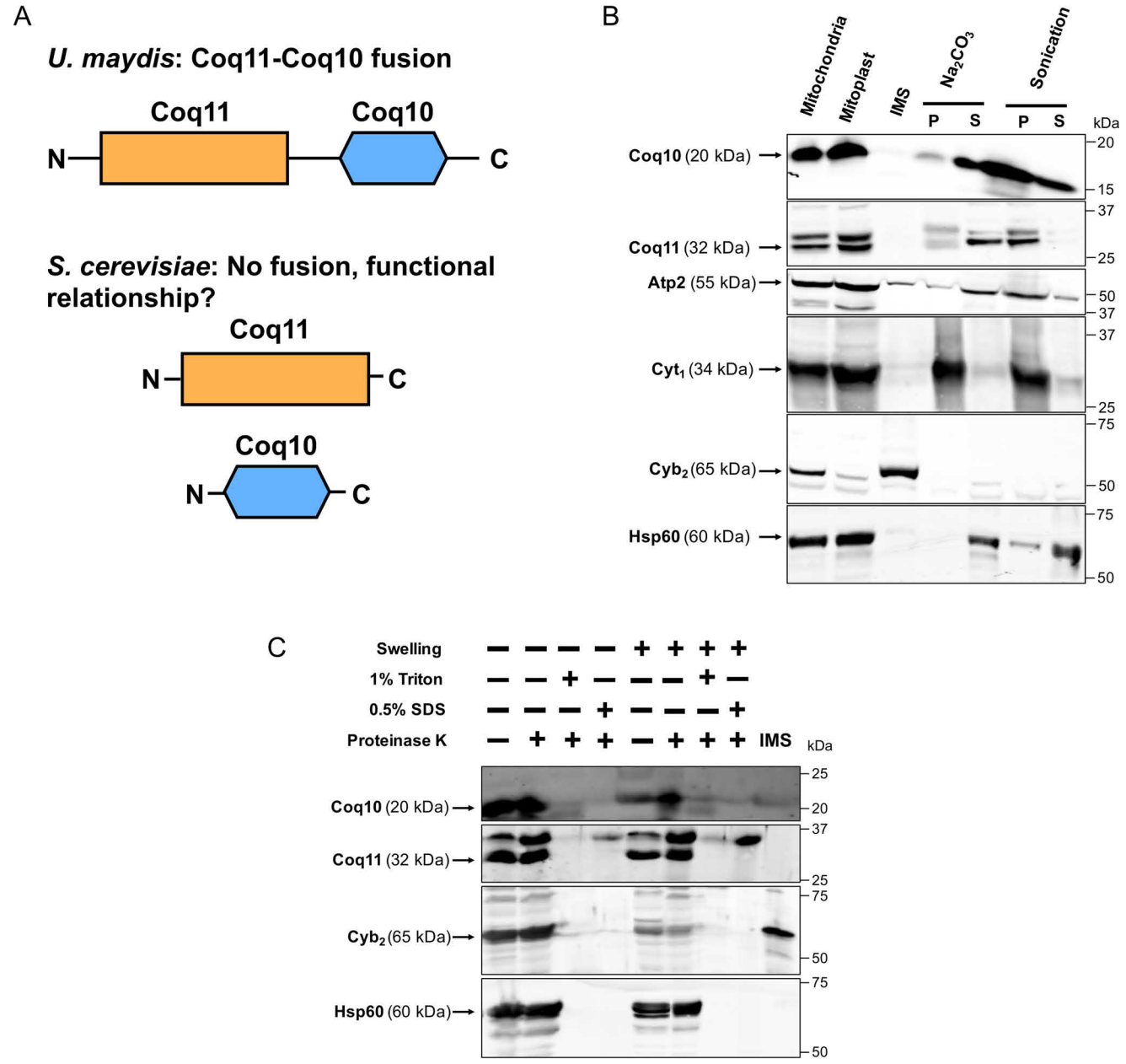

Figure 1. Coq11 and Coq10 are peripherally associated with the mitochondrial inner membrane facing the matrix, and Coq10 is additionally found in the mitochondrial matrix. *A*, Coq10 and Coq11 are fused in multiple fungi, suggesting an evolutionarily functional relationship between these proteins, although they are not found fused in *S. cerevisiae*. *B*, *S. cerevisiae* mitochondria purified from yeast strains cultured on YPGal medium were subjected to hypotonic swelling and centrifugation to separate the IMS proteins from mitoplasts. The mitoplasts were alkaline-treated (Na_2CO_3; pH 11.5) or sonicated and then separated by centrifugation (100,000 × *g* for 1 h) into supernatant (S) or pellet (P) fractions. *C*, intact mitochondria or mitoplasts were treated with 100 μg/ml proteinase K for 30 min on ice, with or without detergent. Mitochondrial polypeptide markers are as follows: *Atp2*, peripheral inner membrane protein; *Cyb*$_2$, intermembrane space protein; *Cyt*$_1$, integral inner membrane protein; and *Hsp60*, soluble matrix protein. Results are representative of two experiments.

its putative role as a START domain protein possessing a hydrophobic cavity to bind and chaperone Q_6 from its site of synthesis to complex III for respiration (17, 18). We hypothesize that dual mitochondrial matrix localization occurs when Coq10 is tightly bound to protein partners to decrease its hydrophobicity.

For better insight into the membrane association of Coq10 and Coq11, intact mitochondria or mitoplasts were treated with proteinase K in the absence or presence of two individual detergents (1% Triton X-100 or 0.5% SDS). Coq10 and Coq11 were both protected from protease treatment in purified mitochondria and mitoplasts, as was the matrix marker Hsp60 (Fig. 1*C*). When protease was used in the presence of either detergent in mitochondria or mitoplasts, all proteins became sensitive to the protease and were degraded. Expanding on the subfractionation results, these data indicate that Coq10 and Coq11 polypeptides are peripherally associated with the inner membrane facing the matrix side in yeast mitochondria, and Coq10 is also found in the mitochondrial matrix itself. The mitochondrial peripheral membrane association of these two proteins is also in agreement with their submitochondrial localization previously identified in a study of the yeast mitochondrial proteome (30).

Table 1
Genotype and source of yeast strains

Strain	Genotype	Source
W303-1B	MAT α *ade2-1 his3-1,15 leu2-,112trp1-1 ura3-1*	R. Rothstein[a]
BY4742	MAT α *his3Δ0 leu2Δ0 met15Δ0 ura3Δ0*	53
JM6	*MAT a his-4* ρ^0	68
JM8	*MAT* α *ade-1* ρ^0	68
BY4742 *coq1*Δ	MAT α *his3Δ0 leu2Δ0 met15Δ0 ura3Δ0 coq1::KanMX4*	69
BY4741 *coq2*Δ	MAT **a** *his3Δ0 leu2Δ0 met15Δ0 ura3Δ0 coq2::KanMX4*	69
BY4742 *coq3*Δ	MAT α *his3Δ0 leu2Δ0 met15Δ0 ura3Δ0 coq3::KanMX4*	69
BY4742 *coq4*Δ	MAT α *his3Δ0 leu2Δ0 met15Δ0 ura3Δ0 coq4::KanMX4*	69
BY4742 *coq5*Δ	MAT α *his3Δ0 leu2Δ0 met15Δ0 ura3Δ0 coq5:: KanMX4*	69
BY4741 *coq6*Δ	MAT **a** *his3Δ0 leu2Δ0 met15Δ0 ura3Δ0 coq6::KanMX4*	Dharmacon, Inc.
BY4742 *coq7*Δ	MAT α *his3Δ0 leu2Δ0 met15Δ0 ura3Δ0 coq7::KanMX4*	69
BY4742 *coq8*Δ	MAT α *his3Δ0 leu2Δ0 met15Δ0 ura3Δ0 coq8::KanMX4*	69
BY4742 *coq9*Δ	MAT α*his3Δ0 leu2Δ0 met15Δ0 ura3Δ0 coq9::KanMX4*	69
BY4742 *coq10*Δ	MAT α *his3Δ0 leu2Δ0 met15Δ0 ura3Δ0 coq10::KanMX4*	69
BY4742 *coq11*Δ	MAT α *his3Δ0 leu2Δ0 met15Δ0 ura3Δ0 coq11::LEU2*	This work
BY4742 *coq10*Δ*coq11*Δ	MAT α *his3Δ0 leu2Δ0 met15Δ0 ura3Δ0 coq10::HIS3 coq11::LEU2*	This work
W303 *coq10*Δ	MAT α *ade2-1 his3-1,15 leu2-3,112trp1-1 ura3-1 coq10::HIS3*	18
W303 *coq10*Δ	MAT **a** *ade2-1 his3-1,15 leu2-3,112trp1-1 ura3-1 coq10::HIS3*	18
W303 *coq10*rev	MAT α *ade2-1 his3-1,15 leu2-3,112trp1-1 ura3-1 coq10::HIS3 sup*	This work
MB-10	Diploid produced from W303 **a** *coq10*Δ x W303 α *coq10*Δrev	This work
W303 *coq11*Δ	MAT α *ade2-1 his3-1,15 leu2-3,112trp1-1 ura3-1 coq11::LEU2*	This work
W303 *coq10*Δ*coq11*Δ	MAT α *ade2-1 his3-1,15 leu2-3,112trp1-1 ura3-1 coq10::HIS3 coq11::LEU2*	This work
BY4741 *cor1*Δ	MAT **a** *his3Δ0 leu2Δ0 met15Δ0 ura3Δ0 cor1::KanMX4*	69

[a] Gift from Dr. Rodney Rothstein Department of Human Genetics, Columbia University.

coq10Δ respiratory defect is alleviated by deletion of COQ11

Based on similar mitochondria localization and genetic evolutionary evidence, a putative functional relationship between Coq10 and Coq11 was further probed using a series of *coq10* and *coq11* single- and double-knockout mutants. Strain descriptions are listed in Table 1. The Coq10 polypeptide is required for respiration in yeast, and mutants lacking *coq10* have poor growth on nonfermentable carbon sources, including YPGlycerol, hereafter referred to as "YPG" (18). Unlike deletion of *COQ10*, *coq11*Δ mutants are respiratory-capable and have comparable growth to WT on nonfermentable carbon sources (14). When *COQ11* was deleted in a *coq10*Δ mutant in two different yeast genetic backgrounds, the sickly growth of *coq10*Δ on nonfermentable YPG was rescued (Fig. 2*A*).

Quantitative respiratory capacity of each mutant was evaluated with an XF96 Extracellular Flux Analyzer (Fig. 2, *B* and *C*). Representative and normalized traces of oxygen consumption rates (OCR) of four independent experiments performed in nonrepressive medium (YPGal) are shown in Fig. 2*B*. Basal rates of OCR were measured prior to the addition of any small molecule inhibitors. Consistent with its slow growth on nonfermentable medium, the *coq10*Δ mutant had a low rate of basal oxygen consumption compared with WT ($p = 0.052$) (Fig. 2*C*). Basal OCR was rescued in the *coq10*Δ*coq11*Δ double mutant (Fig. 2*C*). Following the addition of two sequential injections of FCCP, a mitochondrial oxidative phosphorylation uncoupler, maximal respiration was also quantified. The maximal respiration of *coq10*Δ*coq11*Δ was rescued to that of WT (Fig. 2*C*). These results show that the deletion of *COQ11* in a *coq10*Δ mutant confers a beneficial effect, such that both growth on respiratory medium and OCR are rescued to WT.

Deletion of COQ11 rescues PUFA sensitivity of the coq10Δ mutant

PUFA autoxidation is initiated by the radical-mediated abstraction of vulnerable hydrogen atoms at bis-allylic positions (31). The ensuing carbon-centered radical adds to molecular oxygen to form a lipid peroxyl radical that propagates lipid peroxidation, with the resulting lipid hydroperoxides ultimately driving cellular toxicity (32). The *coq10*Δ mutant is sensitive to treatment with exogenous PUFAs (Fig. 2*D*) (17, 19), likely because the Q_6 chaperone function of Coq10 is required for the antioxidant function of Q_6. Attenuated respiration in *coq10*Δ is rescued in the *coq10*Δ*coq11*Δ double knockout (Fig. 2, *A–C*), presumably through regained function of Q_6 in the electron transport chain. To test whether the antioxidant capability of Q_6 is also restored in the *coq10*Δ*coq11*Δ mutant, yeast strains were evaluated for sensitivity to added PUFAs (Fig. 2*D*). As anticipated, all strains were resistant to treatment with the monounsaturated oleic acid (Fig. 2*D*). Q_6-less *coq9*Δ was sensitive to α-linolenic acid due to the lack of Q_6 antioxidant protection (Fig. 2*D*). Conversely, the Q_6-replete yet respiratory-deficient *cor1*Δ remained resistant to α-linolenic acid (Fig. 2*D*). Deletion of *COQ11* rescued the α-linolenic acid sensitivity of the *coq10*Δ mutant, suggesting that the double knockout has restored Q_6 antioxidant protection (Fig. 2*D*) despite the absence of Coq10 as a Q_6 chaperone.

Independent coq10 revertant with rescued growth on respiratory medium harbors a mutation within COQ11

Although the *coq10*Δ mutant is unable to grow robustly on nonfermentable medium, an earlier study identified a spontaneous *coq10* revertant (*coq10*rev) that arose when *coq10*Δ yeast was cultured for several weeks on nonfermentable medium containing ethanol and glycerol as carbon sources (18). Characterization of this revertant revealed a suppressor mutation within the *COQ11* ORF, resulting in a truncated Coq11 protein that is predicted to be nonfunctional (Fig. 3*A*). This mutation was further assessed for dominance to determine whether it was sufficient to explain the respiratory competence of *coq10*rev. A haploid *coq10*Δ mutant crossed with haploid *coq10*rev produced diploid MB-10 (Table 1), which was capable of growth on respiratory medium (Fig. 3*B*). Illustrated growth

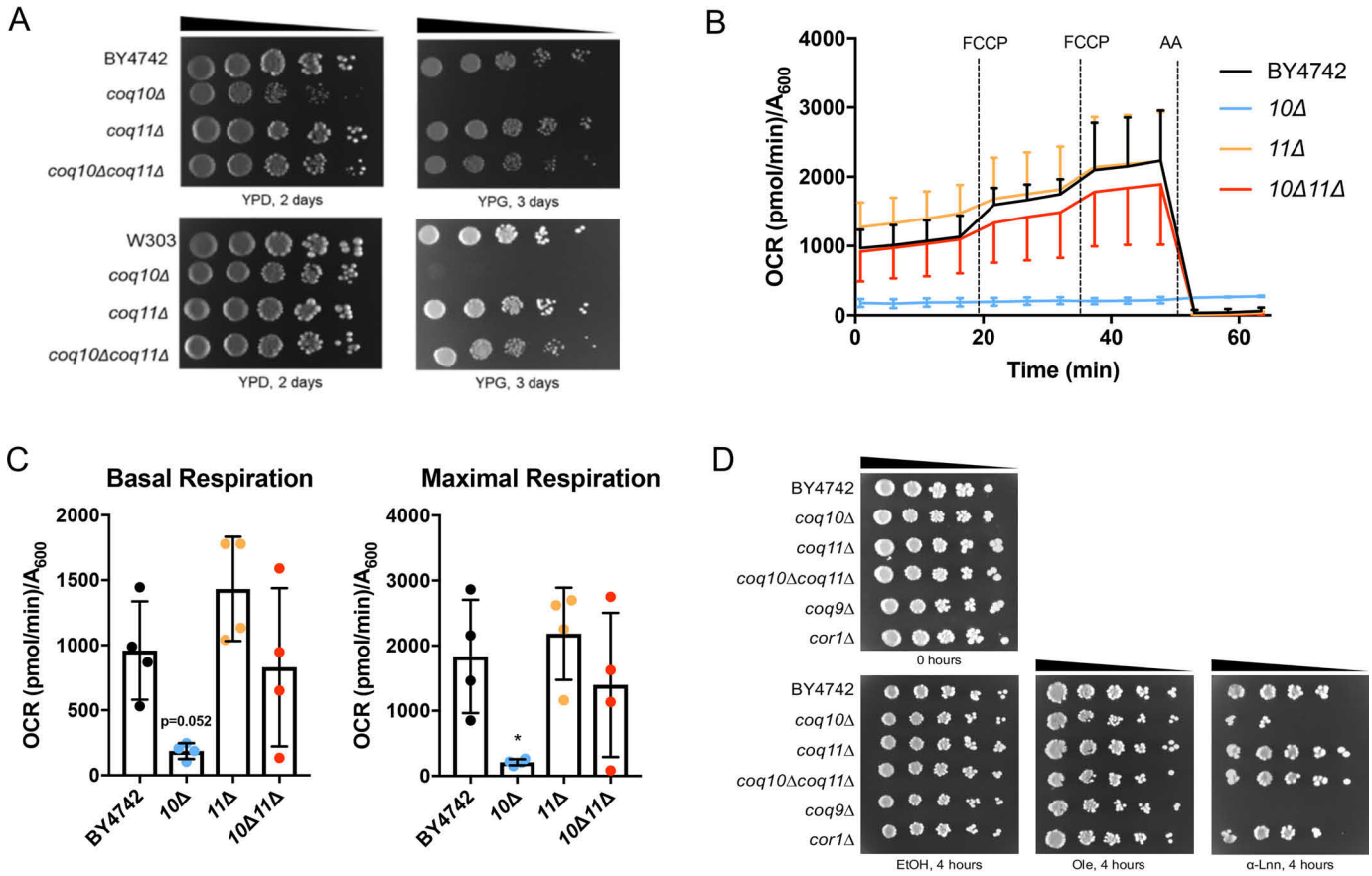

Figure 2. *COQ11* deletion rescues the lack of growth on YPG, low-oxygen consumption rates, and lost Q_6 antioxidant protection in the *coq10Δ* mutant. *A*, strains were grown overnight in 5 ml of YPD, diluted to an A_{600} = 0.2 with sterile PBS, and 2 μl of 5-fold serial dilutions were spotted onto fermentable (YPDextrose, *YPD*) or respiratory (YPGlycerol, *YPG*) medium, corresponding to a final A_{600} = 0.2, 0.04, 0.008, 0.0016, and 0.00032. Plates were incubated at 30 °C, and growth was captured after 2 or 3 days. *B* and *C*, quadruplicates of 25-ml cultures of WT, *coq10Δ*, *coq11Δ*, and *coq10Δcoq11Δ* yeast were grown in YPGal until they reached A_{600} ~4. Yeast were diluted to an A_{600} = 0.1 in fresh YPGal and collected by centrifugation on poly-D-lysine-coated Seahorse XF96 microplates to assess oxygen consumption. *B*, representative traces of OCR of yeast strains with the XF96 extracellular flux analyzer. FCCP and antimycin A (*AA*) were sequentially added to evaluate mitochondrial respiratory states. Measurements were taken approximately every 4 min, as represented by *points* and their respective *error bars*. Four independent experiments were performed (Fig. S1), and each group of average traces represents 8–10 technical replicates. *C*, quantification of basal and maximal (maximal electron transport activity induced by the uncoupler FCCP) OCR as obtained from four independent experiments (Fig. S1). The data show the mean ± S.D., and the statistical significance as compared with WT is represented by *, $p < 0.05$. *D*, deletion of *COQ11* in the *coq10Δ* rescues PUFA sensitivity. Results are representative of three experiments.

patterns suggest that the *coq11* truncated allele present in *coq10*rev is a dominant-negative mutation. Because the dominant mutation in *coq10*rev restores growth on respiratory medium via a functionally suppressive Coq11 truncation mutation, this mutant effectively validates the *coq10Δcoq11Δ* phenotype in an independent system.

Deletion of COQ11 fails to fully restore coq10Δ Q_6 biosynthesis in whole cells

When a *coq* mutant displays anemic growth on respiratory medium, it is often indicative of inefficient Q_6 biosynthesis (7, 9); yeast lacking *COQ10* exhibit both poor growth on respiratory medium and decreased Q_6 biosynthesis in log phase whole cells (17, 19). Although the *coq11Δ* mutant retains the ability to grow on nonfermentable medium, it is also characterized by impaired Q_6 biosynthesis (14). Only a small amount of Q_6 is required for growth on respiratory medium, ~0.2–3% of the total Q_6 found in WT (9, 33, 34). Because the *coq10Δcoq11Δ* double mutant has rescued respiration, we wanted to assess whether recovered growth was accompanied by increased Q_6 biosynthesis. Whole-cell *de novo*–synthesized $[^{13}C_6]Q_6$ and $[^{12}C]Q_6$ were measured in yeast by feeding the quinone ring-labeled precursor, $[^{13}C_6]$4HB, or EtOH vehicle control (Fig. 4). These analyses were performed in the fermentable, nonrepressive YPGal medium (35) to match the conditions of experiments involving purified mitochondria.

Consistent with previous results (14, 17), *coq10Δ* and *coq11Δ* had significantly decreased *de novo*-synthesized $[^{13}C_6]Q_6$ and $[^{12}C]Q_6$ compared with WT (Fig. 4*A*). The *coq10Δ* mutant had a lower total Q_6 content ($[^{13}C_6]Q_6$ + $[^{12}C]Q_6$) than WT and also a lower total Q_6 than *coq11Δ* (Fig. 4*B*). Deletion of *COQ11* in *coq10Δ* yeast led to a slight increase in *de novo*-synthesized $[^{13}C_6]Q_6$ and unchanged $[^{12}C]Q_6$ compared with *coq10Δ* (Fig. 4*A*). Therefore, the *coq10Δcoq11Δ* double mutant presented total Q_6 contents that were significantly lower than either WT or *coq11Δ* (Fig. 4*B*). Given the robust growth of the *coq10Δcoq11Δ* double mutant on YPG, restored respiration, and resistance to PUFA treatment, the low Q_6 concentrations observed are surprising.

Next, we quantified the concentrations of key Q_6-intermediates in the same whole-cell yeast pellets. As shown previously

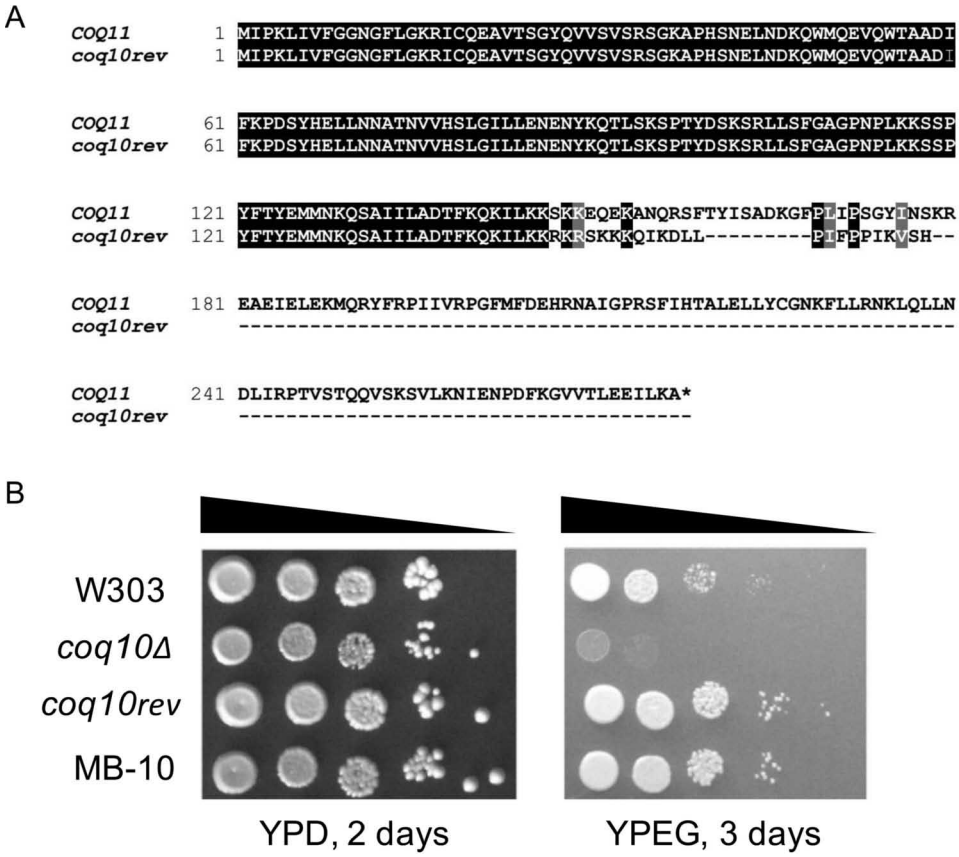

Figure 3. Spontaneous *coq10* revertant with rescued respiratory capacity was identified to possess a base-pair deletion in *COQ11*, encoding a truncated Coq11 protein. *A*, alignment of the amino acid sequence of WT *COQ11* ORF with the *coq11* allele (*coq10rev*) present in the *coq10* revertant. *B*, growth properties of WT were compared with *coq10* mutants and diploid MB-10 (defined in Table 1). Strains were grown overnight in 8 ml of YPDextrose (*YPD*), diluted to an $A_{600} = 0.2$ with sterile PBS, and 2 μl of 5-fold serial dilutions were spotted onto fermentable YPD or respiratory (YPEGlycerol (*YPEG*)) medium, corresponding to a final $A_{600} = 0.2$, 0.04, 0.008, 0.0016, and 0.00032. Plates were incubated at 30 °C, and growth was captured after 2 or 3 days. Results are representative of three experiments.

(17, 19), the *coq10*Δ mutant contained lower amounts of the late-stage intermediate [$^{13}C_6$]DMQ$_6$ and [^{12}C]DMQ$_6$ (Fig. 4*C*) than WT, and it accumulated the early-stage intermediate [$^{13}C_6$]HHB and [^{12}C]HHB (Fig. 4*D*). In contrast to *coq10*Δ, the *coq11*Δ mutant mirrored WT production of both *de novo*-synthesized and unlabeled early- and late-stage intermediates (Fig. 4, *C* and *D*), as shown previously (14). Q$_6$-intermediate trends in *coq10*Δ*coq11*Δ matched those of the *coq10*Δ mutant rather than *coq11*Δ (Fig. 4, *C* and *D*). The low Q$_6$ content and accumulation of early-stage Q$_6$-intermediates in the *coq10*Δ*coq11*Δ double knockout suggest the absence of *COQ10* still produces a notable effect on Q$_6$ biosynthesis, although respiratory capacity is rescued.

*coq10*Δ*coq11*Δ *double mutant has increased mitochondrial Q$_6$ compared with the coq10*Δ *single mutant*

Although Q$_6$ biosynthesis solely occurs within mitochondria, it is found in all cellular membranes (9). Therefore, Q$_6$ was quantified in both whole cells and purified mitochondria from mutant and WT cells cultured under the same conditions (36). Whole-cell Q$_6$ determined under mitochondrial purification conditions matched those determined in Figs. 4 and 5*A*. The *coq10*Δ*coq11*Δ double mutant made slightly more Q$_6$ than the *coq10*Δ single mutant, but overall less Q$_6$ compared with the *coq11*Δ single mutant. All mutants had lower whole-cell Q$_6$ amounts than WT (Fig. 5*A*).

Similarly, mitochondrial Q$_6$ content per microgram of mitochondrial protein was lower in *coq11*Δ than WT (Fig. 5*B*). However, deletion of *COQ11* in the *coq10*Δ mutant increased the mitochondrial Q$_6$ 5-fold (Fig. 5*B*). Despite these profound differences in mitochondrial Q$_6$ content, mitochondrial mass was consistent between strains as determined by three distinct assays (Fig. 5, *C–E*). Increased mitochondrial Q$_6$ in the *coq10*Δ*coq11*Δ double mutant compared with *coq10*Δ indicates that the absence of *COQ11* in part rescues defective Q$_6$ synthesis in the *coq10*Δ mutant.

*Low Coq protein content and destabilized CoQ synthome of the coq10*Δ *mutant are restored in the coq10*Δ*coq11*Δ *double mutant*

Proper formation of the CoQ synthome from component Coq polypeptides is required for efficient Q$_6$ biosynthesis in yeast (9, 12, 13). Deletion of *COQ10* causes a decrease in several other Coq polypeptides, including Coq3–Coq7, Coq9, as well as overall CoQ synthome destabilization (12, 13, 19). These results were confirmed when purified mitochondria from *coq10*Δ yeast were analyzed for each Coq polypeptide (Fig. 6*A*). The *coq10*Δ mutant had significantly decreased amounts of Coq3,

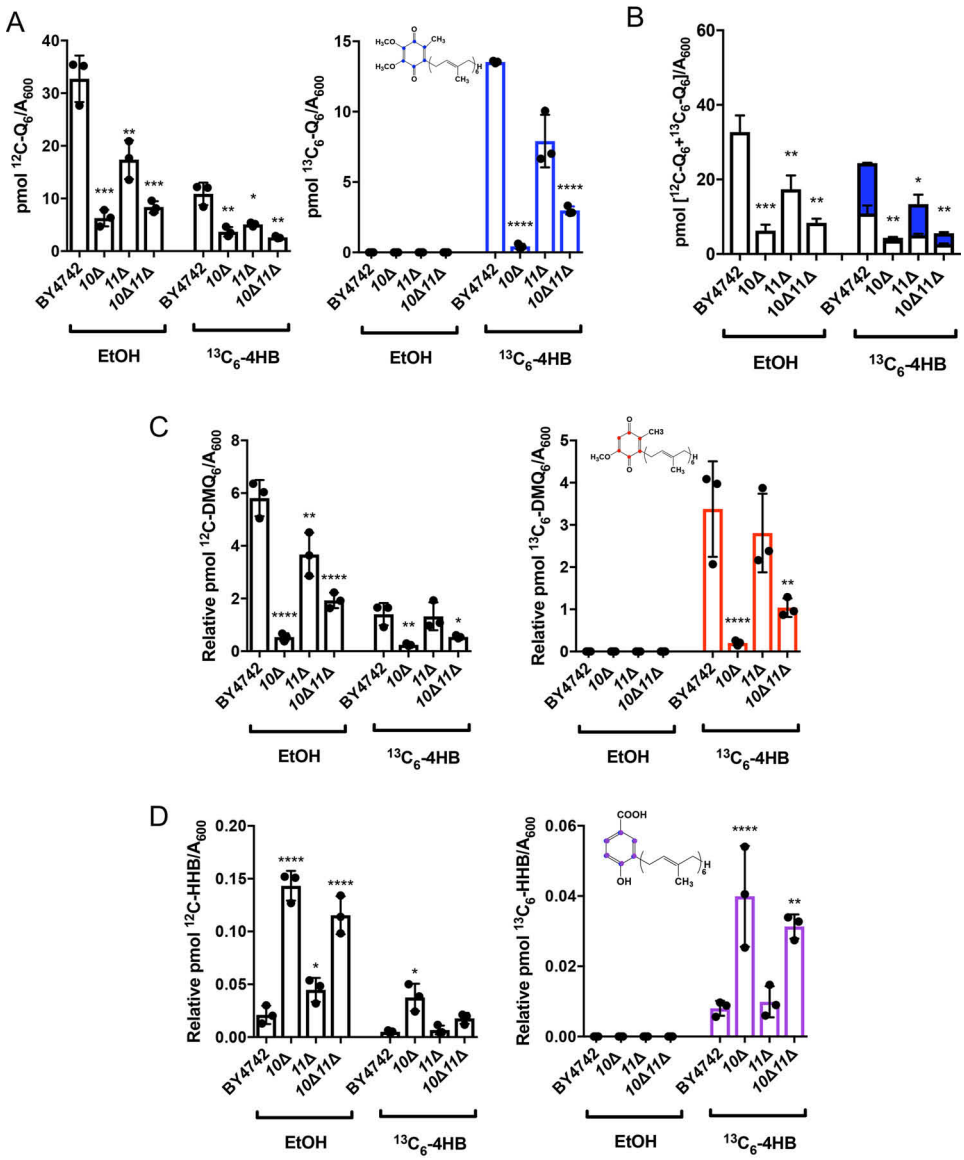

Figure 4. Low amounts of *de novo* [$^{13}C_6$]Q_6 in whole-cell lipid extracts of the *coq10*Δ mutant are only partially restored by deletion of *COQ11*. Triplicates of 6-ml cultures in YPGal were labeled at A_{600} ~1 with 5 μg/ml [$^{13}C_6$]4HB or EtOH vehicle control, and 5 ml of each culture were collected after 4 h, lipid-extracted, and analyzed by LC-MS/MS. *A*, unlabeled [^{12}C]Q_6 and *de novo*–synthesized [$^{13}C_6$]Q_6 (*blue*); *B*, total amount of Q_6 determined from the sum of [$^{13}C_6$]Q_6 and [^{12}C]Q_6; *C*, [^{12}C]DMQ_6 and [$^{13}C_6$]DMQ_6 (*red*); and *D*, [^{12}C]HHB and [$^{13}C_6$]HHB (*purple*) were measured from the whole-cell lipid extracts of WT and the *coq10*Δ, *coq11*Δ, and *coq10*Δ*coq11*Δ mutants. Values are the mean of three replicates. The data show mean ± S.D., and the statistical significance as compared with WT is represented by *, $p < 0.05$; ***, $p < 0.001$; and ****, $p < 0.0001$.

Coq4, Coq7, and Coq9 compared to and plotted as a percentage of WT (Fig. 6*B*).

In contrast to *coq10*Δ, the *coq11*Δ single mutant had elevated Coq4, Coq6, Coq7, and Coq9 (Fig. 6*A*), with protein quantification shown in Fig. 6*B*. Furthermore, the *coq10*Δ*coq11*Δ double mutant also had raised amounts of Coq4, Coq7, and Coq9 polypeptides compared with WT (Fig. 6, *A* and *B*). This increase in Coq proteins could not be explained by enhanced *COQ* transcription as there was no corresponding change in the concentration of the respective mRNAs, (Fig. 6*C*), although *COQ4* mRNA was not detected.

CoQ synthome formation was probed using two-dimensional blue native/SDS-PAGE (2D-BN/SDS-PAGE) with Coq4 and Coq9 serving as sensitive indicators of a high-molecular-weight complex (13). As expected, the CoQ synthome in WT yeast presented as a heterogeneous high-molecular-weight complex, spanning a range of ~140 kDa to >1 MDa for Coq4 (Fig. 7*A*) and from ~100 kDa to >1 MDa for Coq9 (Fig. 7*B*). Consistent with prior results (13, 19), the *coq10*Δ mutant displayed a highly-destabilized CoQ synthome, with a disappearance of large complexes that were replaced by lower-molecular-weight subcomplexes less than ~440 kDa for Coq4 (Fig. 7*A*) and less than ~232 kDa for Coq9 (Fig. 7*B*). The *coq11*Δ mutant had a stabilized CoQ synthome compared with WT, with high-molecular-weight complexes shifting to the left and collapsing into a more homogeneous complex spanning ~900 kDa to >1 MDa for both Coq4 (Fig. 7*A*) and Coq9 (Fig. 7*B*). When *COQ11* was deleted in combination with *COQ10*, there was a substantial rescue of high-molecular-weight complex formation compared with the *coq10*Δ single mutant (Fig. 7, *A* and *B*). The CoQ

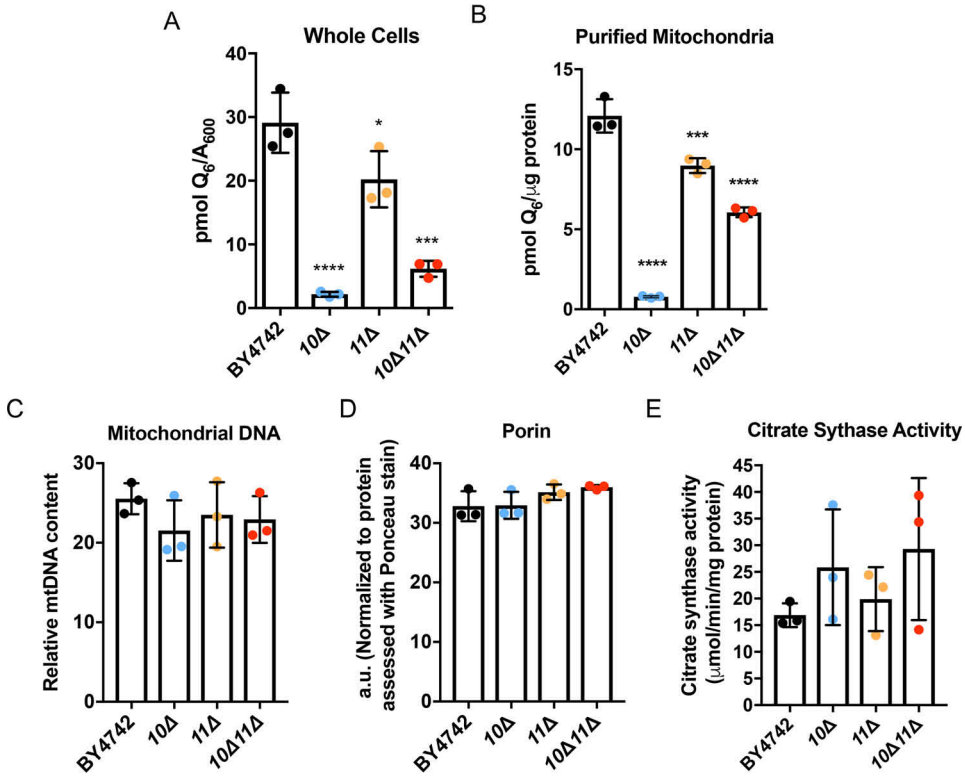

Figure 5. Deletion of *COQ11* in the *coq10*Δ mutant enhances mitochondrial Q_6 content. Triplicates of 30-ml cultures of WT, *coq10*Δ, *coq11*Δ, and *coq10*Δ*coq11*Δ yeast were grown in YPGal until they reached A_{600} ~4. *A*, 5 ml of whole cells from each culture were harvested, lipid-extracted, and analyzed by LC-MS/MS for Q_6 content. Alternatively, WT, *coq10*Δ, *coq11*Δ, and *coq10*Δ*coq11*Δ yeasts were grown in YPGal until they reached A_{600} ~4 and were subjected to mitochondrial preparation. *B*, lipids from triplicates of purified mitochondria (100 μg) were analyzed by LC-MS/MS for Q_6 content. *C–E*, mitochondrial mass was estimated using three distinct methods. *C*, relative mitochondrial DNA to actin was quantified by qPCR. *D*, porin protein amounts were quantified by hand using ImageStudioLite following immunoblot and normalized to total protein levels evaluated by Ponceau stain. *E*, citrate synthase activity was determined using a colorimetric assay as outlined under "Experimental procedures." Values are the mean of three replicates. The data show the mean ± S.D., and the statistical significance as compared with WT is represented by *, $p < 0.05$; ***, $p < 0.001$; and ****, $p < 0.0001$.

synthome of the *coq10*Δ*coq11*Δ double mutant appeared similar to that of *coq11*Δ complexes spanning ~66 kDa to > 1 MDa for Coq4 (Fig. 7*A*) and from ~66 kDa to > 1 MDa for Coq9 (Fig. 7*B*). However, the deletion of *COQ11* in *coq10*Δ does not negate the effect from the *COQ10* deletion, as it does not restore small subcomplexes <140 kDa to higher molecular weights (Fig. 7, *A* and *B*). These CoQ synthome signals for *coq11* mutants were complementary to the observed increased Coq polypeptides, indicating that the absence of *COQ11* enhanced the Q_6 biosynthetic machinery.

High-copy COQ8 does not restore Q_6 content in the coq10Δcoq11Δ single mutant

The Coq8 polypeptide is a member of an ancient atypical kinase family (37), with several conserved kinase motifs that are essential for Q biosynthesis (13, 38). Prior studies have demonstrated that overexpression of Coq8 in a *coq10*Δ mutant increased the otherwise low amounts of several key Coq polypeptides and stabilized CoQ synthome formation (13). This is similar to the phenotype observed when *COQ11* was deleted in the *coq10*Δ mutant. Furthermore, Coq8 overexpression has also been shown to influence Q_6 biosynthesis, including the restoration of late-stage Q_6-intermediates in *coq5–coq9* null mutants (39). Although the CoQ synthome of the *coq10*Δ mutant was stabilized by deletion of *COQ11*, Q_6 and late-stage Q_6-intermediates remained lower compared with WT and the *coq11*Δ single mutant (Fig. 4*C*). We hypothesized that the overexpression of Coq8 in the *coq10*Δ and *coq10*Δ*coq11*Δ mutant may restore Q_6 content in both mutants.

WT, *coq10*Δ, *coq11*Δ, and *coq10*Δ*coq11*Δ were analyzed for growth on nonfermentable medium and Q_6 biosynthesis upon transformation with high-copy *COQ8* (hc*COQ8*, Table 2) or empty vector control (Fig. 8). Similar to previous observations in a different yeast genetic background (18), *coq10*Δ-expressing hc*COQ8* regained the ability to grow on respiratory medium (Fig. 8*A*). This growth phenotype may be explained by a stabilized CoQ synthome in the *coq10*Δ mutant harboring hc*COQ8* (13). However, hc*COQ8* had no material effect on the growth properties of WT, *coq11*Δ, or *coq10*Δ*coq11*Δ strains on YPG (Fig. 8*A*).

Each strain was grown in minimal selection medium to maintain plasmid expression and was analyzed for Q_6 biosynthesis following metabolic labeling with the ring-labeled Q_6 precursor, [$^{13}C_6$]HB (Fig. 8, *B* and *C*). Changing the growth medium from rich (*i.e.* YPGal) to minimal synthetic (*i.e.* SD and dropout dextrose media (DOD)) changed the relative amounts of Q_6 content among the mutants (Figs. 4*B versus* 8*C*). Although WT [$^{13}C_6$]Q_6 and total Q_6 content is similar in Figs. 4*B* and 8*C*, the values for *coq11*Δ and the double mutant are quite different. When grown in YPGal, *coq10*Δ had the lowest Q_6 content, followed by the double mutant *coq10*Δ*coq11*Δ, with *coq11*Δ hav-

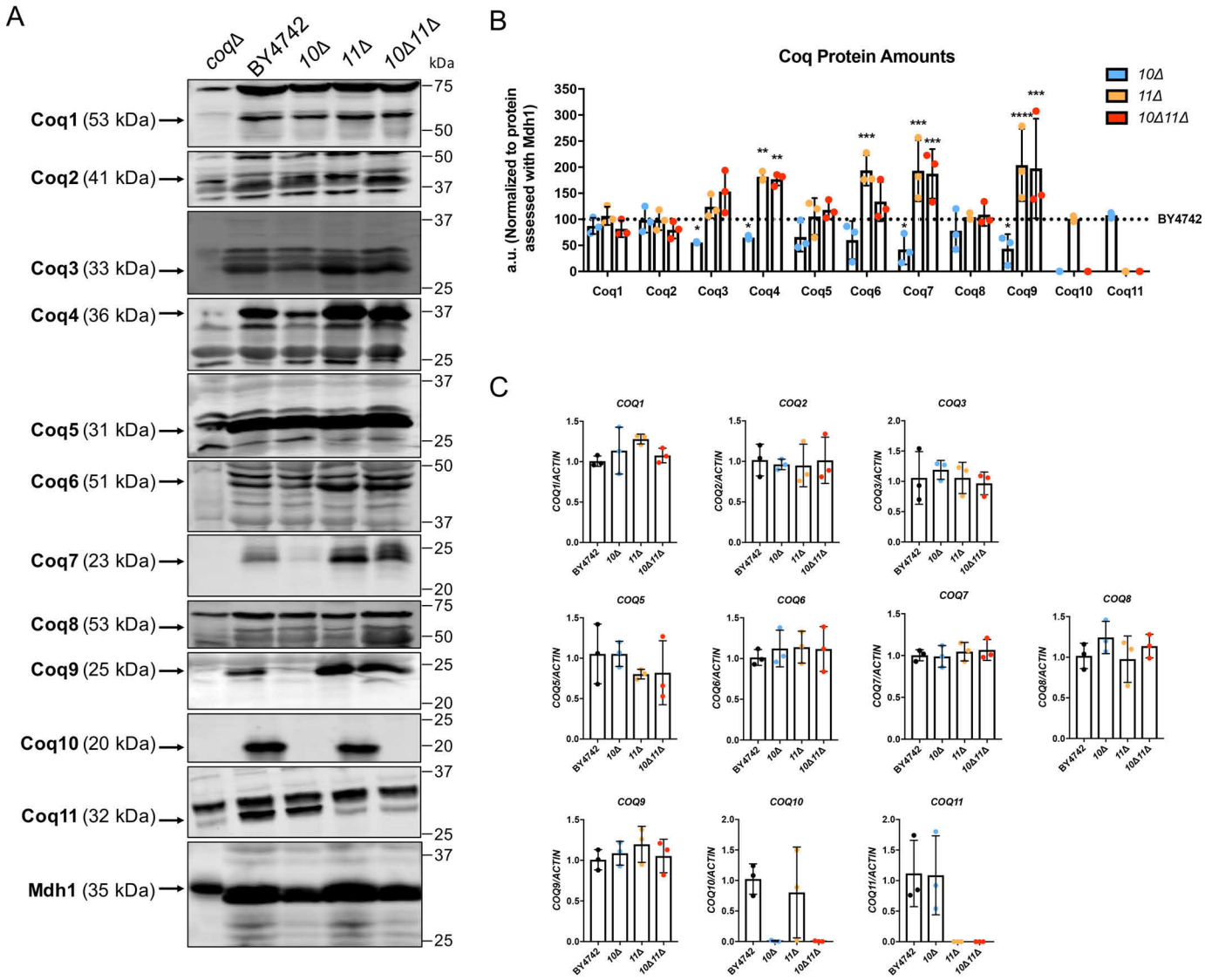

Figure 6. Several Coq polypeptides have increased abundance in *coq11*Δ and *coq10*Δ*coq11*Δ mutants compared with WT. *A*, aliquots of purified mitochondria (25 μg) from WT, *coq10*Δ, *coq11*Δ, and *coq10*Δ*coq11*Δ yeasts were subjected to 10 or 12% Tris-glycine SDS-PAGE. Mitochondrial malate dehydrogenase (Mdh1) was included as a loading control, with a representative blot shown. The Coq5 protein also serves as a qualitative loading control, because the Coq5 polypeptide amounts remain unchanged across the panel of *coq1*–*coq4* and *coq6*–*coq10* deletion mutants (12). Aliquots of purified *coq*Δ mitochondria (*coq1*Δ–*coq11*Δ) were included as negative controls for immunoblotting with antisera to each of the Coq polypeptides. *Black arrows* highlight the location of each protein on the membrane. *B*, ImageStudioLite was used to quantify triplicates of each Coq protein band's intensity by hand, which were normalized to Mdh1 and plotted as a percentage of WT. The data show mean ± S.D., and the statistical significance is as compared with WT is represented by *, $p < 0.05$; **, $p < 0.01$; ***, $p < 0.001$; and ****, $p < 0.0001$. *C*, qPCR was used to determine *COQ* gene expression from whole-cell cultures of WT, *coq10*Δ, *coq11*Δ, or *coq10*Δ*coq11*Δ, and data were normalized to actin. *COQ* RNA levels remain unchanged in the *coq10*Δ, *coq11*Δ, or *coq10*Δ*coq11*Δ mutants as compared with WT.

ing the closest Q_6 content to WT (Figs. 4, *A* and *B*, and 5*A* and Fig. S2, *A* and *B*). In contrast, when these strains are cultured in SD−Ura (Fig. 8, *B* and *C*), the double mutant *coq10*Δ*coq11*Δ had the lowest Q_6 content, as compared with either the *coq10*Δ or *coq11*Δ single mutant strains. Growth on minimal dextrose medium in the absence of plasmid selection produced similar trends (Fig. S2, *C* and *D*, and Fig. S3, *A* and *B*).

Upon Coq8 overexpression, *coq10*Δ had increased *de novo*-synthesized $[^{13}C_6]Q_6$ and $[^{12}C]Q_6$ (Fig. 8*B*), and total Q_6 concentrations ($[^{13}C_6]Q_6 + [^{12}C]Q_6$) were restored to those of WT (Fig. 8*C*). This finding is consistent with previous results, which also indicated that hc*COQ8* restored Q biosynthesis and amounts of Coq polypeptides and the CoQ synthome in the *coq10*Δ mutant (13, 17, 18). Intriguingly, expression of hc*COQ8* had no effect on *de novo* or unlabeled Q_6 content in either the *coq11*Δ single mutant or the *coq10*Δ*coq11*Δ double mutant (Fig. 8*B*). Total Q_6 contents of both *coq11*Δ and *coq10*Δ*coq11*Δ remained significantly decreased compared with WT (Fig. 8*C*). Together, these results show that the rescue of the *coq10*Δ mutant mediated by Coq8 overexpression requires Coq11.

*Expression of low-copy COQ11 rescues only some of the phenotypes of the coq10*Δ*coq11*Δ *mutant*

The functional complementation of *coq11*Δ single and *coq10*Δ*coq11*Δ double mutants with low-copy *COQ11* was assessed (lc*COQ11*, Table 2). As expected, the *coq10*Δ mutant, *coq10*Δ with empty vector, and *coq10*Δ complemented with lc*COQ11* showed slow growth on the nonfermentable carbon

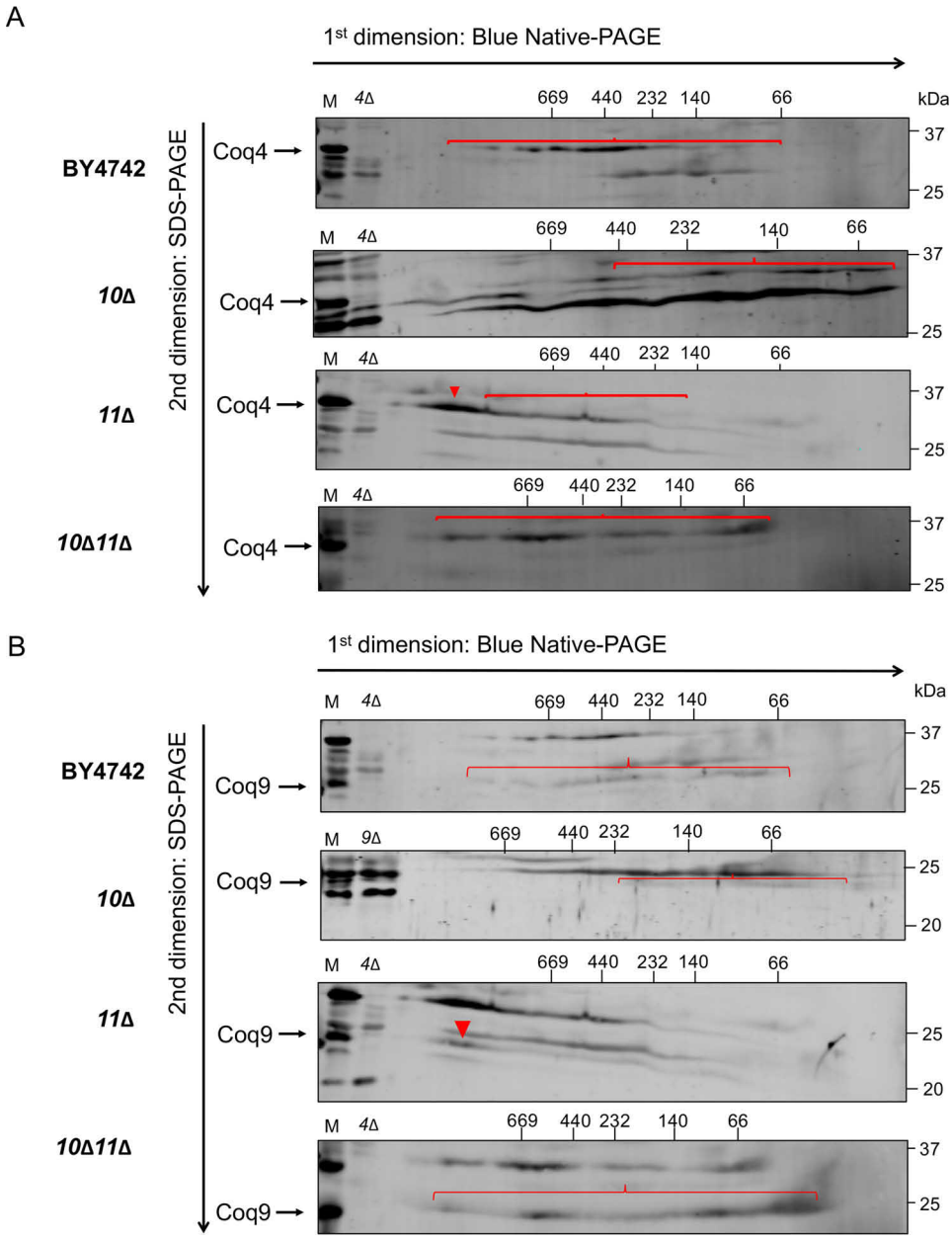

Figure 7. Deletion of *COQ11* in the *coq10*Δ mutant restores the CoQ synthome. Aliquots (100 μg) of purified mitochondria from WT, *coq10*Δ, *coq11*Δ, and *coq10*Δ*coq11*Δ yeasts cultured in YPGal were solubilized with digitonin and separated with two-dimensional BN/SDS-PAGE. Following transfer of proteins to membranes, the CoQ synthome was visualized as a heterogeneous signal from ~66 to ~669 kDa in WT control with antibodies to *A*, Coq4, or *B*, Coq9. Intact mitochondria (25 μg) from each designated strain was included as a loading control (*M*). Aliquots of *coq4*Δ- or *coq9*Δ-purified mitochondria (25 μg) were included as a negative control for the antisera to Coq4 and Coq9, as the Coq9 polypeptide is absent from the *coq4*Δ mutant. *Red arrowheads* and *brackets* indicate distinct complexes.

Table 2
Yeast expression vectors

Plasmid	Relevant genes/markers	Source
pRS305	Yeast vector with *LEU2* marker	70
pRS313	Yeast vector with *HIS3* marker	70
pRS316	Yeast shuttle vector; low-copy	70
lc*COQ11*	pRS316 with yeast *COQ11*; low-copy	This work
pRS426	Yeast shuttle vector; multi-copy	71
p4HN4	pRS426 with yeast *COQ8*; multi-copy	12

source YPGlycerol (Fig. 9*A*). Because yeast lacking *COQ11* retain respiratory capacity (Fig. 2) (14), *coq11*Δ complemented with lc*COQ11* had no detectable change in growth phenotype compared with either the *coq11*Δ mutant or *coq11*Δ with empty vector (Fig. 9*A*). Intriguingly, when lc*COQ11* was expressed in the *coq10*Δ*coq11*Δ double mutant, there was no repression of growth on YPG compared with that of the *coq10*Δ mutant (Fig. 9*A*).

This observation suggests that Q_6 biosynthesis in *coq10*Δ *coq11*Δ may not be affected by lc*COQ11*. To determine the effect of lc*COQ11* expression on mutant Q_6 biosynthesis, yeast was grown in selection medium to maintain plasmid expression. We tested whether lc*COQ11* expression rescued Q_6 content in the *coq11*Δ mutant. Expression of lc*COQ11* in *coq11*Δ efficiently rescued total Q_6 ($[^{13}C_6]Q_6$ + $[^{12}C]Q_6$) to WT amounts (Fig. 9*B*).

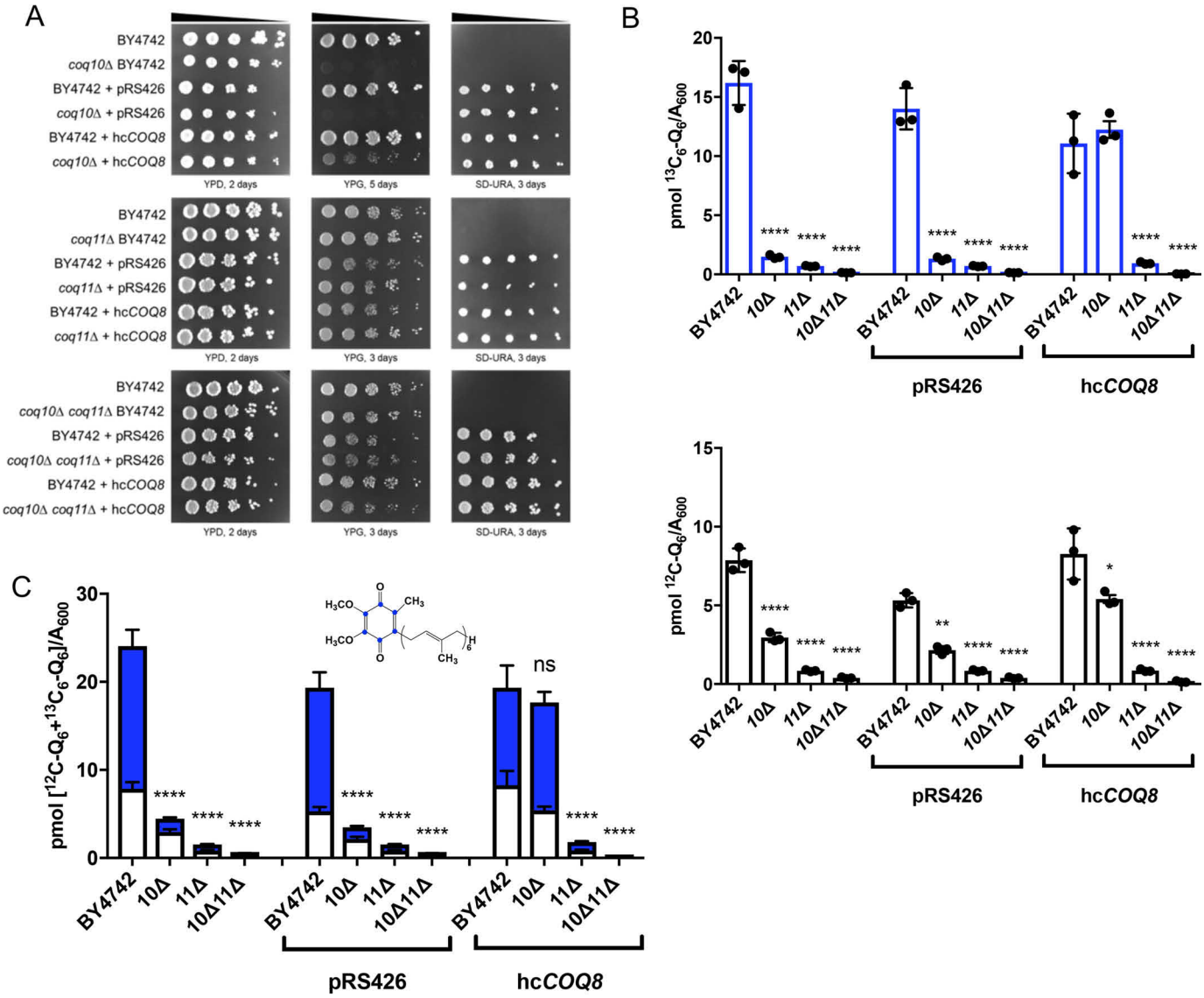

Figure 8. Overexpression of the CoQ synthome stabilizer, *COQ8*, has no effect on Q_6 synthesis in the *coq10Δcoq11Δ* mutant. WT, *coq10*Δ, *coq11*Δ, and *coq10Δcoq11*Δ mutants were transformed with high-copy *COQ8* (hc*COQ8*) or empty vector (pRS426) plasmids. *A*, strains were grown overnight in 5 ml of selection medium, diluted to an A_{600} = 0.2 with sterile PBS, and 2 μl of 5-fold serial dilutions were spotted onto YPD, YPG, or selection medium (SD−Ura), corresponding to a final A_{600} = 0.2, 0.04, 0.008, 0.0016, and 0.00032. Plates were incubated at 30 °C, and growth was captured after 2 or 3 days. Triplicates of 5 ml of culture in selection medium were labeled with 5 μg/ml [$^{13}C_6$]4HB, collected after 4 h, lipid-extracted, and analyzed by LC-MS/MS. *B*, [^{12}C]Q_6 (*white*) and *de novo* [$^{13}C_6$]Q_6 (*blue*). *C*, total amount of Q_6 was also plotted from the sum of [$^{13}C_6$]Q_6 and [^{12}C]Q_6. The values are the means of three replicates. The data show mean ± S.D., and the statistical significance as compared with WT is represented by *, $p < 0.05$; **, $p < 0.01$; ***, $p < 0.001$; and ****, $p < 0.0001$. The *ns* signifies that values are not significantly different from WT.

Finally, whole-cell steady-state Q_6 concentrations were evaluated in all mutants. Even though lc*COQ11* complementation did not suppress *coq10Δcoq11Δ* growth on YPGlycerol (Fig. 9*A*), Q_6 concentrations were increased in *coq10Δcoq11Δ* to a level comparable with that of *coq10*Δ (Fig. 9*C*). This implies that Coq11's role in Q_6 biosynthesis is not effective when the *COQ11* ORF is expressed on a single-copy plasmid in the absence of *COQ10*. Perhaps Coq11 expression from a plasmid does not account for multiple levels of regulation that occur through endogenous expression. Alternatively, the *coq10Δcoq11Δ* double mutant may have slightly lower amounts of the Coq11 polypeptide compared with *coq11*Δ when both are complemented by lc*COQ11* (Fig. 9*D*), and these lower levels may not be sufficient to suppress respiration (Fig. 9*A*).

Discussion

This work investigated a putative functional relationship between Coq10 and Coq11 within the *S. cerevisiae* Q_6 biosynthetic pathway. The presence of Coq10–Coq11 fusions in several Ustilaginaceae species suggests that these proteins may directly interact or participate in the same biological pathway in yeast (Fig. 1*A*) (14). Yeast Coq10 and its orthologs were previously shown to be required for efficient *de novo* Q biosynthesis and respiration (17, 18). We were surprised to discover that the yeast *coq10*Δ growth defect on nonfermentable medium and oxygen consumption rates were rescued upon deletion of *COQ11* (Fig. 2). Moreover, spontaneous revertants isolated from *coq10*Δ yeast were previously found to exhibit growth on

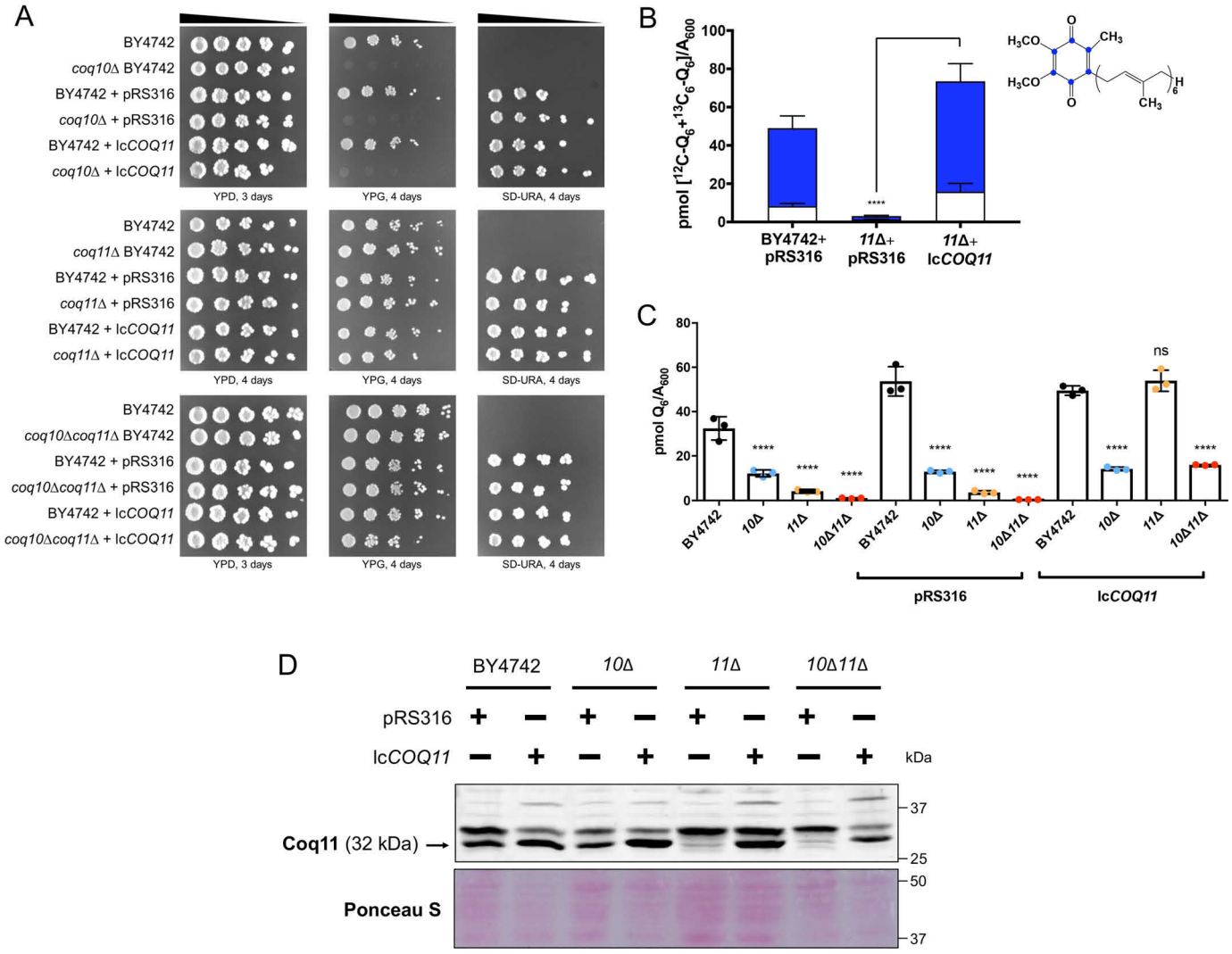

Figure 9. Low-copy *COQ11* rescues only some of the phenotypes of the *coq10Δcoq11Δ* double mutant. A low-copy plasmid expressing *COQ11* (*lcCOQ11*) and an empty vector control (pRS316) were transformed into WT, *coq10Δ*, *coq11Δ*, and *coq10Δcoq11Δ*. *A*, strains were grown overnight in 5 ml of YPDextrose (*YPD*) and diluted to an A_{600} = 0.2 with sterile PBS, and 2 μl of 5-fold serial dilutions were spotted onto YPDextrose, YPGlycerol (*YPG*), or selection medium (SD−Ura), corresponding to a final A_{600} = 0.2, 0.04, 0.008, 0.0016, and 0.00032. Plates were incubated at 30 °C, and growth was captured after 3 or 4 days. *B*, rescue of mutant *de novo* and unlabeled Q_6 production was initially demonstrated in *coq11Δ*. Triplicates of 6-ml cultures in selection medium were labeled with 5 μg/ml [$^{13}C_6$]4HB, and 5 ml of each culture was collected after 4 h, lipid-extracted, and analyzed by LC-MS/MS. Total amount of Q_6 was plotted from the sum of *de novo* [$^{13}C_6$]Q_6 (*blue*) and unlabeled [^{12}C]Q_6. Values are the mean of three replicates. *C*, rescue of mutant Q_6 content was evaluated in each mutant strain. Triplicates of 6-ml cultures in selection medium were grown until A_{600} ~4. Lipid extracts from 5 ml of each culture were analyzed by LC-MS/MS. The data show the means ± S.D., and the statistical significance as compared with WT is represented by *, $p < 0.05$; **, $p < 0.01$; ***, $p < 0.001$; and ****, $p < 0.0001$. *ns* signifies that values are not significantly different from WT. *D*, aliquots of purified mitochondria (25 μg) from WT and mutant yeast containing empty vector or lc*COQ11* were isolated in YPGal medium and were separated on 10% Tris-glycine SDS-polyacrylamide gels to determine Coq11 protein expression. Proteins stained with Ponceau stain were used as loading control.

nonfermentable medium (18). We have shown that this reversion is due to a dominant base pair deletion within the *COQ11* gene, likely resulting in a nonfunctional, truncated Coq11 protein (Fig. 3). Mutants lacking both *COQ10* and *COQ11* when cultured on YPGal have increased *de novo* Q_6 production (Fig. 4*A*) in addition to a 5-fold increase in mitochondrial Q_6 content compared with the *coq10Δ* single knockout (Fig. 5*B*). Therefore, we have demonstrated that deletion of the Coq11 polypeptide in a *coq10Δ* mutant confers a beneficial effect on both respiration and Q_6 biosynthesis (Fig. 10).

Enhanced Q_6 content in the *coq10Δcoq11Δ* double mutant compared with the *coq10Δ* single mutant may be partially due to increased amounts of several key Coq polypeptides (Fig. 6) and CoQ synthome stabilization (Fig. 7). The ring-modifying enzymes within the Q_6 biosynthetic pathway colocalize to numerous distinct "CoQ domains" *in vivo*, and proper assembly of the CoQ synthome components is required for the presence of these CoQ domains (23). Two recent studies demonstrated that mitochondria isolated from yeast lacking *COQ10* have a reduced number of CoQ domain puncta (23, 24). This is likely due to lower levels of certain Coq polypeptides and partial CoQ synthome destabilization in the *coq10Δ* mutant (17, 19), which was confirmed in this work (Figs. 6 and 7). In contrast, *coq11Δ* yeast displayed significantly higher amounts of Coq4, Coq6, Coq7, and Coq9 polypeptides (Fig. 6). The CoQ synthome was likewise shifted to a higher molecular weight in *coq11Δ* mitochondria compared with WT (Fig. 7). When Coq9–yEGFP was used as a marker for CoQ domains, *coq11Δ* had increased CoQ

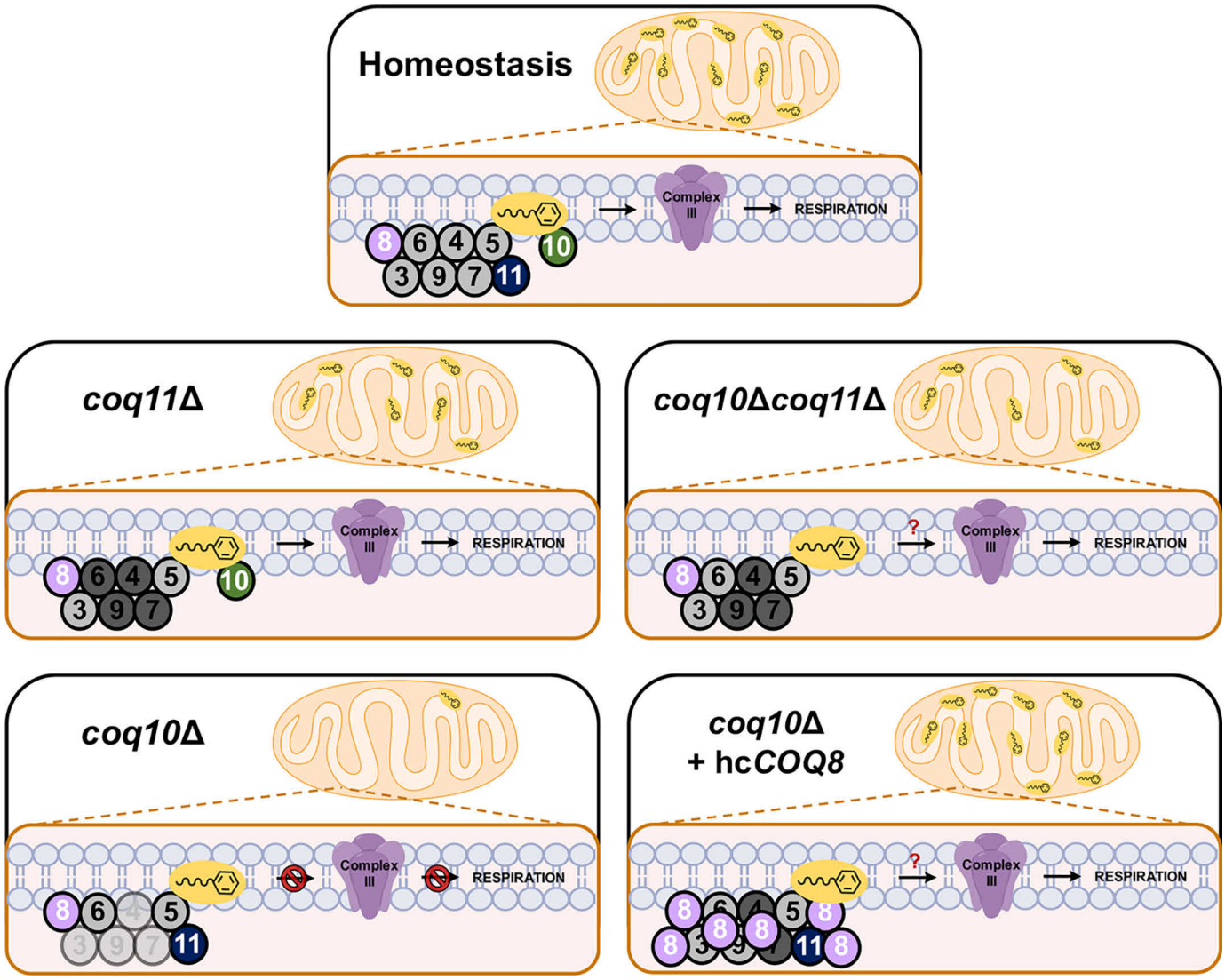

Figure 10. Scheme postulating Coq11 as a modulator of Q_6 synthesis in mitochondria. Under homeostasis, Coq11 associates with the CoQ synthome and acts as a modest negative regulator of Q_6 synthesis via Coq10. In the absence of *COQ11*, several Coq polypeptides are increased (*dark shading*), and the CoQ synthome is stabilized compared with WT cells, despite a slight decrease in Q_6 content. In contrast, the *coq10*Δ mutant is missing the Q_6 chaperone protein, resulting in a decreased amount (*light shading*) of Coq3, Coq4, Coq7, and Coq9, a destabilized CoQ synthome, substantially decreased Q_6 concentrations, and a lack of respiration. The deletion of *COQ11* in the *coq10*Δ mutant counterbalances the destabilized CoQ synthome and decreased Q_6 content phenotype of the *coq10*Δ mutant, allowing the *coq10*Δ*coq11*Δ double mutant to grow on YPG and respire. Expression of hc*COQ8* in the *coq10*Δ mutant produces many similar phenotypes to *COQ11* deletion in *coq10*Δ cells, including increased Coq polypeptides and a stabilized CoQ synthome (13), resulting in restored growth on YPG. Unlike the *coq10*Δ*coq11*Δ double mutant, *coq10*Δ + hc*COQ8* has rescued Q_6 content pointing to an additional role of Coq11 in Q_6 biosynthesis, redox regulation, or transportation.

domain intensity that stemmed from amplified expression of Coq9–yEGFP, although the number of domains was similar to WT. Mutants lacking essential Coq polypeptides *coq1*–*coq9*, or *coq10*, displayed significantly less Coq9-labeled domains (24). The CoQ synthome stabilization seen in *coq11*Δ via 2D-BN/SDS-PAGE analyses performed in this work (Fig. 7) agrees with the observation of increased CoQ domains and argues that the CoQ synthome is truly stabilized upon deletion of *COQ11*, as opposed to inducing a greater number of domains.

These observations are consistent with the biochemical data that led to the notion of a CoQ synthome whose formation relies on the presence of prenylated Q-intermediates (13, 40, 41). The *coq10*Δ mutant produced more early-stage intermediates (HHB) and had less late-stage intermediates (DMQ_6) compared with WT (Fig. 4, *C* and *D*), resulting in less CoQ synthome formation (Fig. 7). Because *coq11*Δ yeast displayed comparable amounts of early- and late-stage Q_6-intermediates to WT (Fig. 4, *C* and *D*), this mutant retained the ability to fully form the CoQ synthome (Fig. 7). The double knockout synthesized varying amounts of early- and late-stage Q_6-intermediates that were largely in-between those of the single knockouts (Fig. 4, *C* and *D*). The CoQ synthome is thus able to form in *coq10*Δ*coq11*Δ yeast, albeit not to the efficiency of the *coq11*Δ single mutant (Fig. 7). We suspect that the accumulation of Coq polypeptides and restoration of the CoQ synthome in the *coq10*Δ*coq11*Δ double mutant are sufficient to allow for Q_6 to escape its site of synthesis and reach the respiratory complexes, despite an absence of the Coq10 Q_6 chaperone protein and lower Q_6 in this strain (Fig. 10). How this occurs is presently not known. One possible explanation could be that Coq11 inhibits

a currently unidentified Q_6 chaperone with lower efficiency than Coq10 that is able to rescue respiration only in the absence of both Coq10 and Coq11.

Overexpression of the Q_6-biosynthetic protein Coq8 also rescued *coq10*Δ mutant growth on nonfermentable medium (Fig. 8*A*) and *de novo* Q_6 biosynthesis (Fig. 8, *B* and *C*) (17). Coq8 has been implicated in the partial extraction of Q_6-intermediates out of the mitochondrial inner membrane for enzymatic modification by other Coq proteins, allowing for appropriate Q_6 biosynthesis (25). Prior investigations also revealed that Coq8 overexpression in *coq10*Δ yeast increased Coq4 and Coq9 polypeptides and stabilized the CoQ synthome (13, 24). Despite the substantial benefit of Coq8 overexpression in a *coq10*Δ single mutant, Coq8 overexpression failed to enhance Q_6 biosynthesis in the *coq10*Δ*coq11*Δ double knockout (Figs. 8, *B* and *C*, and 10). The absence of *COQ11* in the double mutant is sufficient to restore Coq polypeptides and CoQ synthome formation (Figs. 6, *A* and *B*, 7, and 10). Coq11 and Coq8 may therefore work by different mechanisms to serve opposing functions for CoQ synthome and Coq polypeptide stabilization. Furthermore, it is clear that Coq11 is required to perform an additional function to Coq8, as hc*COQ8* requires the presence of Coq11 to restore Q_6 biosynthesis (Figs. 8, *B* and *C*, and 10).

Proper CoQ synthome formation is not only required for efficient Q_6 biosynthesis, but it is also vital for the establishment of ER-mitochondrial contact sites mediated by the ER-mitochondrial encounter structure (ERMES) complex (23, 24). The ERMES complex is essential for lipid exchange between the ER and mitochondria (42). Specifically, *ERMES* null mutants have irregular Q_6 cellular distribution and a destabilized CoQ synthome (23). When *COQ10* was deleted in yeast expressing Coq6–GFP, there was a significant decrease in Coq6–GFP puncta colocalization with Mdm34–mCherry, a component of the ERMES complex (23). These results indicate that CoQ synthome positioning next to the ERMES complex, and subsequent Q_6 distribution from the mitochondria, depends on Coq10. Because *COQ11* deletion stabilizes the CoQ synthome (Figs. 6, *A* and *B*, and 7), it is possible that *coq11*Δ mutants have more ER-mitochondrial contacts through the ERMES complex and improved transfer of lipids between these organelles. Therefore, one possible role of Coq11 may be an auxiliary protein mediating lipid transport between the ER and mitochondria.

In a recent study, Coq11 was named Mrx2, as part of the mitochondrial organization of gene expression (MIOREX) complex involved in the mitochondrial genetic expression system (43). Considering the proposed regulatory function of Coq11 in CoQ synthome assembly, it is tempting to speculate that Coq11 offers a mechanism to couple Q_6 synthesis with the assembly of the respiratory complexes. When the synthesis of the respiratory complexes is more active, Coq11 is associated to the MIOREX complex, and Q_6 synthesis at ER junctions is stimulated. Coq11 dual localization in the mitochondrial inner membrane, to the MIOREX complex and the CoQ synthome, would also explain the sensitivity of yeast cells to the number of *COQ11* copies, as well as present another example of a loop system control for balanced expression of mitochondrial products (44).

Another potential explanation for the phenotypes induced by the knockout of Coq11 relates to its structural connection with the short-chain dehydrogenase/reductase (SDR) superfamily of NAD(P)(H)-dependent oxidoreductases (14, 45). These enzymes catalyze an assortment of reactions, including isomerization, decarboxylation, epimerization, imine reduction, and carbonyl–alcohol oxidoreduction (45). SDR superfamily proteins contain a conserved protein structural motif known as a Rossmann fold, a feature used in the binding of nucleotide cofactors such as FAD, FMN, and NAD(P) (46). The crystal structure of the *Pseudomonas aeruginosa* gene UbiX, which catalyzes the decarboxylation step in Q_9 biosynthesis, revealed a Rossmann fold with a bound FMN (47). Thus, Coq11 may use its Rossmann fold in conjunction with a nucleotide cofactor to perform similar redox chemistry in *S. cerevisiae* Q_6 biosynthesis. The ratio of QH_2/Q serves as a metabolic sensor for electron transport chain efficiency (48). High QH_2/Q ratios induce respiratory complex I-mediated reverse electron transport (RET) under physiological conditions in both *Drosophila* and mammalian cell lines (48, 49). Superoxide and secondary reactive species produced specifically through complex I RET extended *Drosophila* lifespan and improved mitochondrial function in a model of Parkinson's disease (49). RET induced by over-reduction of the Q pool presumably generates a superoxide-dependent signal essential for homeostasis, such that manipulation of the Q redox state is beneficial for mitochondrial function (48, 49). Mitochondrial phenotypes in the absence of *COQ11*, including restored respiration in *coq10*Δ *coq11*Δ and up-regulated Q_6 machinery (Figs. 2, *A–C*, 6, and 7), seem to correlate well with the aforementioned effects of Q_6H_2 accumulation. Yeast *coq11*Δ and *coq10*Δ*coq11*Δ mutants retain antioxidant protection by Q_6H_2, demonstrated by their resistance to treatment with exogenously-added PUFAs (Fig. 2*D*). Because cells lacking the Coq11 polypeptide maintain Q_6H_2 as an antioxidant, it follows that Coq11 could be involved in the oxidation of Q_6H_2 to Q_6.

The phenotypes of Coq10 and Coq11 seen in this work are similar to those in both fungi and mammalian hosts. Several fungi use Coq11 or Coq11-like proteins as NAD-dependent epimerases/dehydratases, NADH-ubiquinone oxidoreductases, and NADH dehydrogenase subunits (14). Coq11 orthologs are commonly found in plant and algae genomes, including the chloroplast-localized flavin reductase protein At1g32220 from the land plant *Arabidopsis thaliana*, which is thought to be involved in plastoquinone biosynthesis and storage (14, 50). The closest but distinct higher eukaryotic Coq11-like protein is the SDR subfamily protein NDUFA9 (14), an auxiliary subunit of complex I in humans (51). Patients with decreased NDUFA9 expression are unable to properly assemble complex I and may develop a degenerative infancy respiratory disorder known as Leigh syndrome (52). Although yeast cells do not possess complex I, this evidence indicates that Coq11 may play a crucial role in respiratory regulation or function, supporting the observations of this study.

The function of Coq10 is widely conserved across different organisms. Expression of the Coq10 homolog from *C. crescentus* (CC1736) rescues the impaired respiration and antioxidant function of Q_6 in *coq10* yeast mutants (17). The NMR structure

of CC1736 reveals a START domain, which is known to bind lipids via a hydrophobic tunnel (20). Studies of *S. pombe* Coq10 demonstrate that it is able to bind Q_{10} (21). One proposed function of Q binding by CC1736 and Coq10 from *S. pombe* may be to regulate Q delivery to its proper sites in the respiratory complexes. Humans have two distinct homologs of yeast Coq10: COQ10A and COQ10B. Expression of either human protein rescues the *coq10*Δ respiratory deficiency and sensitivity to oxidative stress, and it restores the amounts of Coq polypeptides to WT (19). The conserved function of yeast Coq10 with human COQ10A and COQ10B suggests that the findings of this work will shed light on the role of Coq10 as a chaperone in humans, leading to a better understanding of the pathobiology of Q_{10} diseases.

In summary, this work reveals that Coq11 plays a regulatory role to maintain Q_6 homeostasis in concert with Coq10 in *S. cerevisiae* (Fig. 10). The absence of *COQ11* caused an augmentation of Q_6 production and respiration in the *coq10*Δ mutant, indicating that Coq11 confers a negative effect on the CoQ synthome. Coq11 may be crucial for Q_6 function in addition to Q_6 biosynthesis, as total whole-cell and mitochondrial Q_6 content remained lower than WT in *coq11*Δ and *coq10*Δ*coq11*Δ mutants.

Experimental procedures

All reagents were obtained commercially from Thermo Fisher Scientific unless otherwise specified

Yeast strains and growth medium

S. cerevisiae strains used in this study are described in Table 1. Yeast strains were derived from S288C (BY4742 (53)) or W303 (54). Growth media were prepared as described previously (55), and plate medium contained 2% bacto-agar. Growth media included the following: YPD (2% glucose, 1% yeast extract, and 2% peptone), YPGal (2% galactose, 1% yeast extract, 2% peptone, and 0.1% dextrose), YPG (3% glycerol, 1% yeast extract, and 2% peptone), and YPEG (3% glycerol, 2% ethanol, 1% yeast extract, and 2% peptone). Synthetic dextrose/selection media (SD–Complete, SD−Ura, SD-Leu, SD-His, SD-His–Leu, SD−Ura–Leu) were prepared as described previously (55) and consisted of all components minus uracil, leucine, histidine, or both uracil and leucine. Drop-out dextrose (DOD) medium was prepared as described previously (14).

COQ11 was disrupted by the one-step gene replacement method (56). The *LEU2* gene from pRS305 was amplified by polymerase chain reaction (PCR), with *COQ11* upstream and downstream flanking sequences 5′-GGGAAATATGTATCGTATACAAAAATACAGCTAAAGCTTGAACTG and 3′-GTACTTAACTATATACAGCTTGGTATAATTTTAAAATGGTAATAAC. Transformations of PCR products into yeast cells were performed using the Li-acetate method (57). The double *coq10*Δ*coq11*Δ mutant was constructed via disruption of *COQ10* within the *coq11*Δ strain. The *HIS3* gene from pRS313 was amplified by PCR with *COQ10* upstream and downstream flanking sequences 5′-GGATAAGGAGCCAAACAATAAACGGCTAAAGATACCGTGG and 3′-CAGATAACAAAGATCATGCCATCCAGGATAAGCGTATGCA, and transformation was performed as for the *COQ11* disruption. Primers were designed using SnapGene (GSL Biotech, LLC, Chicago, IL).

Mitochondria isolation from BY4742 WT and mutant yeast

Yeast cultures of BY4742, *coq10*Δ, *coq11*Δ, and *coq10*Δ *coq11*Δ were grown overnight in 5 ml of YPD. Yeast-containing plasmids were grown overnight in 5 ml of selection medium (SD−Ura). All pre-cultures were back-diluted with YPGal and grown overnight with shaking (30 °C, 250 rpm) until cell density reached an A_{600} ~4. Spheroplasts were prepared with Zymolyase-20T (MP Biomedicals) and fractionated as described previously (36), in the presence of cOmplete™ EDTA-free protease inhibitor mixture tablets (Roche Applied Science), phosphatase inhibitor mixture set I (Sigma-Aldrich), phosphatase inhibitor mixture set II (Sigma-Aldrich), and phenylmethylsulfonyl fluoride (Thermo Fisher Scientific). Nycodenz (Sigma-Aldrich) density gradient purified mitochondria were frozen in liquid nitrogen, aliquoted, and stored at −80 °C until further use. Protein concentration of mitochondria was measured by the bicinchoninic acid (BCA) assay (Thermo Fisher Scientific).

Submitochondrial localization of Coq10 and Coq11 polypeptides

Purified mitochondria from BY4742 yeast (3 mg of protein, 150 μl) were subfractionated, as described previously (13). Proteinase K treatment of purified BY4742 mitochondria was also performed as described previously (13). Proteinase K-treated mitoplasts and control samples were resuspended in SDS sample buffer (50 mM Tris, pH 6.8, 10% glycerol, 2% SDS, 0.1% bromphenol blue, and 1.33% β-mercaptoethanol); equal aliquots were separated by SDS-gel electrophoresis on 10 or 12% Tris-glycine polyacrylamide gels as detailed below. Several mitochondrial compartment markers and proteins of interest, Coq10 and Coq11, were detected with rabbit polyclonal antibodies prepared in blocking buffer at dilutions listed in Table S1.

Oxygen consumption evaluation by Seahorse

Mitochondrial function was assessed using the XF96 extracellular flux analyzer (Seahorse Bioscience, Agilent Technologies). Seahorse plates were coated with 50 μg/ml poly-D-lysine (Sigma-Aldrich), diluted 1:1 in UltraPure distilled water (Thermo Fisher Scientific). Volumes of 25 μl were added to each well for 30 min at room temperature and then aspirated before plates were dried overnight at room temperature. The Seahorse XF96 sensor cartridge was hydrated with Seahorse XF calibrant solution (Agilent) and was incubated overnight at room temperature.

Yeast cultures of BY4742, *coq10*Δ, *coq11*Δ, and *coq10*Δ*coq11*Δ were grown overnight in 25 ml of YPGal medium. On the day of measurement, all cultures were diluted to seed an $A_{600} = 0.1$ cells/well of BY4742, *coq10*Δ, *coq11*Δ, and *coq10*Δ*coq11*Δ into a Seahorse XF96 microplate in a total volume of 175 μl YPGal. Four wells containing only medium were included for background measurement. The loaded plate was centrifuged at 500 × *g* for 3 min at room temperature (with no brakes). Following centrifugation, the loaded plate was incubated for 30

min at 37 °C with no CO_2 to aid in the transitioning of the plate into the Seahorse machine's temperature. Cells were stimulated sequentially with two injections of 4 μM FCCP in ports A and B (optimized for maximum oxygen consumption rate) (Enzo Life Sciences) and 2.5 μM antimycin A in port C (Enzo Life Sciences), delivered in YPGal. Mix, wait, and measure times were 2 min, 30 s, and 2 min, respectively. Basal respiration included four measurements, and then following each injection three measurements were made. All OCR were subtracted for nonmitochondrial respiration and normalized to A_{600} = 0.1. Basal respiration was calculated as an average of OCR prior to the first FCCP addition. Maximal respiration was calculated as an average of OCR following the second FCCP addition. Nonmitochondrial respiration was measured as average OCR following antimycin A addition.

Fatty acid sensitivity assay

Sensitivity of yeast cells to PUFA-induced oxidative stress was performed as described previously (19, 58, 59), with some modifications. Briefly, BY4742 WT, *cor1*Δ, *coq9*Δ, *coq10*Δ, *coq11*Δ, and *coq10*Δ*coq11*Δ were inoculated in 5 ml of YPD medium and incubated overnight at 30 °C, 250 rpm. Cultures were subinoculated to an A_{600} = 0.25 in 15 ml of fresh YPD medium and incubated at 30 °C, 250 rpm until they reached an A_{600} ~1. Cells were harvested, washed twice with 10 ml of sterile H_2O, and diluted in 0.1 M phosphate buffer with 0.2% dextrose, pH 6.2, to an A_{600} = 0.2. This cell suspension was divided into 5-ml aliquots and treated with an ethanol vehicle control (final concentration 0.1% v/v), ethanol-diluted oleic acid (Nu-Check Prep), or α-linolenic acid (Nu-Check Prep) to a final concentration of 200 μM. Fatty acid-treated cultures were incubated for 4 h at 30 °C, 250 rpm, after which cell viability was assessed via plate dilutions. Cell viability prior to the addition of fatty acids was determined via plate dilutions, represented in the 0-h plate.

Analysis of Q_6 and Q_6-intermediates

Standards of Q_6 were obtained from Avanti Polar Lipids, and Q_4 was from Sigma-Aldrich. Yeast cultures were grown overnight in 30 ml of YPGal, or selection medium (SD-complete or SD−Ura) for strains harboring plasmids. Cultures were diluted into triplicates of 6 ml of fresh medium to A_{600} = 0.5, and 5 ml of medium was harvested by centrifugation once they reached A_{600} ~4. Cell pellets were stored at −20 °C. Following collection, frozen cell pellets were lipid-extracted in the presence of internal standard Q_4 and analyzed for Q_6 and Q_6-intermediates by LC-MS/MS as described previously (19).

Stable isotope labeling for determination of de novo Q_6 and Q_6-intermediates

Yeast cultures were grown overnight in 30 ml of YPGal and diluted in triplicates of 6 ml of fresh medium to an A_{600} = 0.1. Cultures were incubated until they reached an A_{600} ~1, at which point ethanol vehicle control (0.1% v/v) or 5 μg/ml of the stable isotope [$^{13}C_6$]4HB (Cambridge Isotope Laboratories, Inc.) was added. Cultures were allowed to grow for an additional 4 h when 5 ml of each culture was harvested by centrifugation and stored at −20 °C. Cell pellets were lipid extracted and analyzed by LC-MS/MS as described previously (19).

Mitochondrial DNA determination by qPCR analysis

DNA was extracted from yeast cells as follows. Yeast pellets (10 ml) grown in YPGal were collected at an A_{600} ~4 by centrifugation at 3000 × *g* for 5 min, washed with 5 ml of H_2O, and transferred to 2-ml screw-cap tubes. Pellets were frozen at −80 °C until DNA extraction was carried out. Cell pellets were resuspended in 200 μl of lysis buffer (10 mM Tris-Cl, pH 8.0, 2% (v/v) Triton X-100, 1 mM EDTA, 100 mM NaCl, 1% SDS), and 200 μl of acid-washed glass beads with 200 μl of phenol/chloroform/isoamyl alcohol (25:24:1) were added to the cell suspension. Cells were lysed using a bead-beater (Precellys 24; Bertin Technologies) three times for 10 s at 6500 rpm with a 45-s break between rounds at 4 °C. Tris-EDTA (TE, 200 μl) was added, and the cell suspension was centrifuged at 13,000 × *g* for 5 min at room temperature. The aqueous layer was removed to a new tube containing 200 μl of chloroform, mixed by inversion, and centrifuged at 13,000 × *g* for 5 min at room temperature. This was repeated once more. The aqueous layer was then transferred to a 2-ml screw-cap tube containing 1 ml of 95% EtOH, mixed by inversion, and centrifuged at 13,000 × *g* for 2 min at room temperature. The resulting pellet was resuspended in 400 μl of TE containing 30 μg of RNase A and incubated at 37 °C for 30 min. Then, 10 μl of 3 M sodium acetate and 1 ml of 95% EtOH was added, mixed by inversion, and incubated at −20 °C for 1 h. After 1 h at −20 °C, the suspension was centrifuged at 13,000 × *g* for 5 min, and the pellet was washed twice with 70% EtOH and air-dried. The dried pellet was resuspended in 25 μl of TE; concentration was measured by Nanodrop (Thermo Fisher Scientific), and the pellet was stored at −20 °C until use.

qPCR was performed on a CFX384 instrument (Bio-Rad) using the SensiFAST™SYBR® NO ROX kit (Bioline) as per the manufacturer's instructions. Each sample was run in duplicate with 150 ng of total DNA used per reaction using the following thermocycling protocol (95 °C for 2 min, 95 °C for 5 s, 60 °C for 10 s, and 72 °C for 20 s, plate read and cycle repeated ×40, melt curve 40–92 °C with plate read and 40 °C for 10 s). Melting-curve analysis confirmed that all PCRs produced a single product. mtDNA-specific primers (forward (13,999), 5′-GTG CGT ATA TTT CGT TGA TGC GT-3′; reverse (14,297), 5′-TTC ACA CTG CCT GTG CTA TCT AA-3′ (60) and actin-specific primers (forward, 5′-GAA TTG AGA GTT GCC CCA GA-3′; reverse, 5′-ATC ACC GGA ATC CAA AAC AA-3) were used. The relative level of gene expression of mitochondrial DNA was normalized to the expression level of actin as described previously (61).

Citrate synthase activity

The measurement of citrate synthase activity in cells was carried out as described previously (62). Briefly, yeast pellets (10 ml) grown in YPGal were collected at an A_{600} ~4 by centrifugation at 3000 × *g* for 5 min, washed with 5 ml of H_2O, and transferred to 2-ml screw-cap tubes. Cell pellets were resuspended in 200 μl of lysis buffer (100 mM Tris-Cl, pH 7.4, 1% (v/v) Triton X-100, 1 mM EDTA, 1 mM phenylmethylsulfonyl fluoride, 1× cOmplete™ Protease Inhibitor Mixture (Roche

Applied Science)), and then 200 μl of acid-washed glass beads were added. Cells were lysed using a bead-beater (Precellys 24; Bertin Technologies) three times for 10 s at 6500 rpm with a 45-s break between rounds at 4 °C. The clarified cell lysate was collected after centrifugation at 16,000 $\times$ *g* for 10 min at 4 °C. The concentration of protein was determined with the BCA assay (Thermo Fisher Scientific). Cell lysates were normalized to 0.05 μg/μl protein. The colorimetric citrate synthase assay was carried out using a VersaMax plate reader (Molecular Devices) and a flat-bottom 96-well plate. First, 40 μl of 500 mM Tris-Cl, pH 7.4, 2 μl of 30 mM acetyl-CoA, 8 μl of 2.5 mM 5,5′-dithiobis(2-nitrobenzoic acid), 90 μl of H_2O, and 50 μl cell lysate (2.5 μg total protein) were added into each well. Then, 10 μl of 10 mM oxaloacetic acid were added per well and mixed by pipetting up and down. A_{412} was measured every 30 s at 25 °C. The initial slope was calculated by using data from the first 10 min and used to determine the enzyme reaction rate using the extinction coefficient for 2-nitro-5-thiobenzoate of 14.15 mM^{-1} cm^{-1} (63).

Porin quantification

Porin content was quantified via immunoblot of yeast WT and mutant whole cells. Protein extraction from whole cells was performed (64), and 25 μg of each sample was separated by SDS-gel electrophoresis as described below. Three replicates of the immunoblots were performed and quantified by hand using ImageStudioLite software normalized to Ponceau total protein staining.

Quantitative real-time PCR (qRT-PCR)

Total RNA was isolated from yeast cells using TRIzol reagent (Invitrogen). DNA contamination from the resulting RNA was removed using the DNase TURBO kit as per the manufacturer's instructions (Invitrogen). RNA concentration was measured by Nanodrop (Thermo Fisher Scientific), and RNA was stored at −20 °C. Reverse transcription was carried out using the Superscript III first strand synthesis system using random hexamer primers (Invitrogen). cDNA was stored at −20 °C until qPCR analyses were carried out. Quantitative real-time PCR was performed on a CFX384 instrument (Bio-Rad) using the SensiFAST™SYBR® NO-ROX kit (Bioline) in duplicate. The relative levels of gene expression were normalized to the expression level of actin. Melting curve analysis confirmed that all PCRs produced a single product. The primers (forward/reverse) used in real-time PCR were designed using Primer3 on line (RRID: SCR_003139). Primers used are given in Table S2.

SDS-PAGE and immunoblot analysis

Purified mitochondria (25 μg) were resuspended in SDS sample buffer and separated by SDS-gel electrophoresis on 10 or 12% Tris-glycine polyacrylamide gels. Proteins were transferred to a 0.45-μm polyvinylidene difluoride membrane (Millipore) and blocked with blocking buffer (0.5% BSA, 0.1% Tween 20, 0.02% SDS in PBS). Representative Coq polypeptides and loading control mitochondrial malate dehydrogenase (Mdh1) were probed with rabbit polyclonal antibodies prepared in blocking buffer at dilutions listed in Table S1. IRDye 680LT goat anti-rabbit IgG secondary antibody (LiCOR) was used at a dilution of 1:10,000. Proteins were visualized using a LiCOR Odyssey IR Scanner (LiCOR). Immunoblots are representative of three replicates and were quantified by hand using ImageStudioLite software normalized to Mdh1.

Two-dimensional Blue Native/SDS-PAGE immunoblot analysis of high-molecular-weight complexes

2D-BN/SDS-PAGE was performed as described previously (13, 65, 66). Briefly, 200 μg of purified mitochondria were solubilized at 4 mg/ml for 1 h on ice with 16 mg/ml digitonin (Biosynth) in the presence of the protease and phosphatase inhibitors used during mitochondrial isolation. Protein concentration of solubilized mitochondria was determined by BCA assay. NativePAGE 5% G-250 sample additive (Thermo Fisher Scientific) was added to a final concentration of 0.25%. Solubilized mitochondria (100 μg) were separated on NativePAGE 4–16% BisTris gels (Thermo Fisher Scientific) in the first dimension, and native gel slices were further separated on 12% Tris-glycine polyacrylamide gel in the second dimension. Following the second-dimension separation, immunoblot analyses were performed as described above, using antibodies against Coq4 and Coq9 at the dilutions indicated in Table S1. Molecular weight standards for BN gel electrophoresis and SDS gel electrophoresis were obtained from GE Healthcare (Sigma-Aldrich) and Bio-Rad, respectively.

Construction of low-copy COQ11 yeast expression vectors

Plasmids used in this study are described in Table 2. A low-copy *COQ11*-containing plasmid was constructed using the pRS316 low-copy empty vector. The *COQ11* ORF and regions corresponding to 842 bp upstream and 256 bp downstream were cloned into pRS316 using Gibson Assembly (New England Biolabs). Clones were sequenced by Laragen, and successful clones were transformed into WT and mutant yeast, along with the corresponding empty vector (pRS316) control as described above.

Revertant isolation

As reported previously, *coq10* mutant growth deficiency on nonfermentable carbon sources (YPEG) spontaneously revert due to nuclear suppression mutations (18). Here, W303 *coq10*Δ yeast was grown on glucose to stationary phase, and ~10 million cells were plated on YPEG. After several weeks, a colony began to appear on this medium. The colony was purified, and its genome was sequenced.

Genome sequencing

The Wizard® genomic purification kit (Promega) was used to extract total DNA from the parental respiratory-deficient mutant W303 *coq10*Δ and from the spontaneous revertant W303 *coq10*rev. The DNA was quantified using the QUBIT DNA™ high-sensitivity assay, and 1 ng of the normalized DNA was tagged by the Nextera XTTM (Illumina) protocol. The libraries were amplified and pooled as described (67). The pooled libraries were subjected to sequencing with the NextSeq™ (Illumina) equipment in the Genome Investigation and Analysis Laboratory of the Institute of Biomedical Sciences at the University of Sao Paulo. The BWA Aligner tool,

version 1.1.4 (Base Space Labs-Illumina), was used to align ~23,000,000 reads obtained from each strain with the reference genomes of *S. cerevisiae*. The alignments were compared using the Integrative Genomics Viewer (Base Space Labs Illumina).

Statistical analyses

All data sets were tested for normality using GraphPad Prism 7 with the Shapiro-Wilk normality test. Because a majority of sets passed the normality test ($\alpha = 0.5$), statistical analyses were performed using GraphPad Prism 7 with parametric one-way analysis of variance correcting for multiple comparisons using Tukey's test, comparing the mean of each sample to the mean of its corresponding WT or empty vector control. The data show the means ± S.D., and the statistical significance as compared with WT or empty vector control is represented by the following: *, $p < 0.05$; **, $p < 0.01$; ***, $p < 0.001$; and ****, $p < 0.0001$. The denotation *ns* indicates values with "not significant" differences from the corresponding control.

Data availability

The MS source data for determination of Q_6 and Q_6 intermediates will be shared upon request. Please contact Catherine Clarke at cathy@chem.ucla.edu. All remaining data are contained within the article.

Author contributions—M. C. B., M. H. B., and C. F. C. conceptualization; M. C. B., J. N., A. A., H. S. T., O. S. S., M. H. B., and C. F. C. resources; M. C. B., K. Y., L. F.-dR., J. N., A. A., H. S. T., N. A. N., M. H. B., and C. F. C. data curation; M. C. B., J. N., A. A., and M. H. B. software; M. C. B., K. Y., L. F.-dR., J. N., A. A., H. S. T., N. A. N., R. S., M. H. B., and C. F. C. formal analysis; M. C. B., R. S., O. S. S., M. H. B., and C. F. C. supervision; M. C. B., J. N., H. S. T., M. H. B., and C. F. C. funding acquisition; M. C. B., K. Y., L. F.-dR., J. N., A. A., H. S. T., R. S., and M. H. B. validation; M. C. B., K. Y., L. F.-dR., J. N., A. A., H. S. T., N. A. N., R. S., M. H. B., and C. F. C. investigation; M. C. B., K. Y., L. F.-dR., J. N., A. A., H. S. T., N. A. N., M. H. B., and C. F. C. visualization; M. C. B., K. Y., L. F.-dR., J. N., A. A., H. S. T., N. A. N., R. S., M. H. B., and C. F. C. methodology; M. C. B. and C. F. C. writing-original draft; M. C. B., R. S., M. H. B., and C. F. C. project administration; M. C. B., K. Y., L. F.-dR., J. N., A. A., H. S. T., N. A. N., R. S., O. S. S., M. H. B., and C. F. C. writing-review and editing.

Acknowledgments—We thank the UCLA Molecular Instrumentation Core proteomics facility and Dr. Yu Chen for the use of the QTRAP4000 for lipid analysis. We thank undergraduate UCLA researcher Hope Ibarra for her contributions in assisting with experiments.

References

1. Turunen, M., Olsson, J., and Dallner, G. (2004) Metabolism and function of coenzyme Q. *Biochim. Biophys. Acta* **1660,** 171–199 CrossRef Medline
2. Alcázar-Fabra, M., Trevisson, E., and Brea-Calvo, G. (2018) Clinical syndromes associated with coenzyme Q_{10} deficiency. *Essays Biochem.* **62,** 377–398 CrossRef Medline
3. Desbats, M. A., Lunardi, G., Doimo, M., Trevisson, E., and Salviati, L. (2015) Genetic bases and clinical manifestations of coenzyme Q_{10} (CoQ 10) deficiency. *J. Inherit. Metab. Dis.* **38,** 145–156 CrossRef Medline
4. Frei, B., Kim, M. C., and Ames, B. N. (1990) Ubiquinol-10 is an effective lipid-soluble antioxidant at physiological concentrations. *Proc. Natl. Acad. Sci. U.S.A.* **87,** 4879–4883 CrossRef Medline
5. Okada, K., Suzuki, K., Kamiya, Y., Zhu, X., Fujisaki, S., Nishimura, Y., Nishino, T., Nakagawa, T., Kawamukai, M., and Matsuda, H. (1996) Polyprenyl diphosphate synthase essentially defines the length of the side chain of ubiquinone. *Biochim. Biophys. Acta* **1302,** 217–223 CrossRef Medline
6. Kawamukai, M. (2016) Biosynthesis of coenzyme Q in eukaryotes. *Biosci. Biotechnol. Biochem.* **80,** 23–33 CrossRef Medline
7. Stefely, J. A., and Pagliarini, D. J. (2017) Biochemistry of mitochondrial coenzyme Q biosynthesis. *Trends Biochem. Sci.* **42,** 824–843 CrossRef Medline
8. Montini, G., Malaventura, C., and Salviati, L. (2008) Early coenzyme Q_{10} supplementation in primary coenzyme Q_{10} deficiency. *N. Engl. J. Med.* **358,** 2849–2850 CrossRef Medline
9. Awad, A. M., Bradley, M. C., Fernández-Del-Río, L., Nag, A., Tsui, H. S., and Clarke, C. F. (2018) Coenzyme Q_{10} deficiencies: pathways in yeast and humans. *Essays Biochem* **62,** 361–376 CrossRef Medline
10. Tran, U. C., Marbois, B., Gin, P., Gulmezian, M., Jonassen, T., and Clarke, C. F. (2006) Complementation of *Saccharomyces cerevisiae coq7* mutants by mitochondrial targeting of the *Escherichia coli* UbiF polypeptide: two functions of yeast Coq7 polypeptide in coenzyme Q biosynthesis. *J. Biol. Chem.* **281,** 16401–16409 CrossRef Medline
11. Marbois, B., Gin, P., Faull, K. F., Poon, W. W., Lee, P. T., Strahan, J., Shepherd, J. N., and Clarke, C. F. (2005) Coq3 and Coq4 define a polypeptide complex in yeast mitochondria for the biosynthesis of coenzyme Q. *J. Biol. Chem.* **280,** 20231–20238 CrossRef Medline
12. Hsieh, E. J., Gin, P., Gulmezian, M., Tran, U. C., Saiki, R., Marbois, B. N., and Clarke, C. F. (2007) *Saccharomyces cerevisiae* Coq9 polypeptide is a subunit of the mitochondrial coenzyme Q biosynthetic complex. *Arch. Biochem. Biophys.* **463,** 19–26 CrossRef Medline
13. He, C. H., Xie, L. X., Allan, C. M., Tran, U. C., and Clarke, C. F. (2014) Coenzyme Q supplementation or overexpression of the yeast Coq8 putative kinase stabilizes multi-subunit Coq polypeptide complexes in yeast *coq* null mutants. *Biochim. Biophys. Acta* **1841,** 630–644 CrossRef Medline
14. Allan, C. M., Awad, A. M., Johnson, J. S., Shirasaki, D. I., Wang, C., Blaby-Haas, C. E., Merchant, S. S., Loo, J. A., and Clarke, C. F. (2015) Identification of Coq11, a new coenzyme Q biosynthetic protein in the CoQ-synthome in *Saccharomyces cerevisiae*. *J. Biol. Chem.* **290,** 7517–7534 CrossRef Medline
15. Marcotte, E. M., Pellegrini, M., Ng, H. L., Rice, D. W., Yeates, T. O., and Eisenberg, D. (1999) Detecting protein function and protein–protein interactions from genome sequences. *Science* **285,** 751–753 CrossRef Medline
16. Perocchi, F., Jensen, L. J., Gagneur, J., Ahting, U., von Mering, C., Bork, P., Prokisch, H., and Steinmetz, L. M. (2006) Assessing systems properties of yeast mitochondria through an interaction map of the organelle. *PLoS Genet.* **2,** e170 CrossRef Medline
17. Allan, C. M., Hill, S., Morvaridi, S., Saiki, R., Johnson, J. S., Liau, W. S., Hirano, K., Kawashima, T., Ji, Z., Loo, J. A., Shepherd, J. N., and Clarke, C. F. (2013) A conserved START domain coenzyme Q-binding polypeptide is required for efficient Q biosynthesis, respiratory electron transport, and antioxidant function in *Saccharomyces cerevisiae*. *Biochim. Biophys. Acta* **1831,** 776–791 CrossRef Medline
18. Barros, M. H., Johnson, A., Gin, P., Marbois, B. N., Clarke, C. F., and Tzagoloff, A. (2005) The *Saccharomyces cerevisiae COQ10* gene encodes a START domain protein required for function of coenzyme Q in respiration. *J. Biol. Chem.* **280,** 42627–42635 CrossRef Medline
19. Tsui, H. S., Pham, N. V. B., Amer, B. R., Bradley, M. C., Gosschalk, J. E., Gallagher-Jones, M., Ibarra, H., Clubb, R. T., Blaby-Haas, C. E., and Clarke, C. F. (2019) Human COQ10A and COQ10B are distinct lipid-binding START domain proteins required for coenzyme Q function. *J. Lipid Res.* **60,** 1293–1310 CrossRef Medline
20. Shen, Y., Goldsmith-Fischman, S., Atreya, H. S., Acton, T., Ma, L., Xiao, R., Honig, B., Montelione, G. T., and Szyperski, T. (2005) NMR structure of the 18 kDa protein CC1736 from *Caulobacter crescentus* identifies a member of the START domain superfamily and suggests residues mediating substrate specificity. *Proteins* **58,** 747–750 CrossRef Medline

21. Cui, T. Z., and Kawamukai, M. (2009) Coq10, a mitochondrial coenzyme Q binding protein, is required for proper respiration in *Schizosaccharomyces pombe*. *FEBS J.* **276,** 748–759 CrossRef Medline
22. Stoldt, S., Wenzel, D., Kehrein, K., Riedel, D., Ott, M., and Jakobs, S. (2018) Spatial orchestration of mitochondrial translation and OXPHOS complex assembly. *Nat. Cell Biol.* **20,** 528–534 CrossRef Medline
23. Eisenberg-Bord, M., Tsui, H. S., Antunes, D., Fernández-Del-Río, L., Bradley, M. C., Dunn, C. D., Nguyen, T. P. T., Rapaport, D., Clarke, C. F., and Schuldiner, M. (2019) The endoplasmic reticulum–mitochondria encounter structure complex coordinates coenzyme Q biosynthesis. *Contact* **2,** 2515256418825409 CrossRef Medline
24. Subramanian, K., Jochem, A., Le Vasseur, M., Lewis, S., Paulson, B. R., Reddy, T. R., Russell, J. D., Coon, J. J., Pagliarini, D. J., and Nunnari, J. (2019) Coenzyme Q biosynthetic proteins assemble in a substrate-dependent manner into domains at ER-mitochondria contacts. *J. Cell Biol.* **218,** 1353–1369 CrossRef Medline
25. Reidenbach, A. G., Kemmerer, Z. A., Aydin, D., Jochem, A., McDevitt, M. T., Hutchins, P. D., Stark, J. L., Stefely, J. A., Reddy, T., Hebert, A. S., Wilkerson, E. M., Johnson, I. E., Bingman, C. A., Markley, J. L., Coon, J. J., *et al.* (2018) Conserved lipid and small-molecule modulation of *COQ8* reveals regulation of the ancient kinase-like UbiB family. *Cell Chem. Biol.* **25,** 154–165.e11 CrossRef Medline
26. Reading, D. S., Hallberg, R. L., and Myers, A. M. (1989) Characterization of the yeast *HSP60* gene coding for a mitochondrial assembly factor. *Nature* **337,** 655–659 CrossRef Medline
27. Fujiki, Y., Hubbard, A. L., Fowler, S., and Lazarow, P. B. (1982) Isolation of intracellular membranes by means of sodium carbonate treatment: application to endoplasmic reticulum. *J. Cell Biol.* **93,** 97–102 CrossRef Medline
28. Chen, W. J., and Douglas, M. G. (1987) Phosphodiester bond cleavage outside mitochondria is required for the completion of protein import into the mitochondrial matrix. *Cell* **49,** 651–658 CrossRef Medline
29. Ohashi, A., Gibson, J., Gregor, I., and Schatz, G. (1982) Import of proteins into mitochondria. The precursor of cytochrome c_1 is processed in two steps, one of them heme-dependent. *J. Biol. Chem.* **257,** 13042–13047 Medline
30. Vögtle, F. N., Burkhart, J. M., Gonczarowska-Jorge, H., Kücükköse, C., Taskin, A. A., Kopczynski, D., Ahrends, R., Mossmann, D., Sickmann, A., Zahedi, R. P., and Meisinger, C. (2017) Landscape of submitochondrial protein distribution. *Nat. Commun.* **8,** 290 CrossRef Medline
31. Yin, H., Xu, L., and Porter, N. A. (2011) Free radical lipid peroxidation: mechanisms and analysis. *Chem. Rev.* **111,** 5944–5972 CrossRef Medline
32. Pryor, W. A., and Porter, N. A. (1990) Suggested mechanisms for the production of 4-hydroxy-2-nonenal from the autoxidation of polyunsaturated fatty acids. *Free Radic. Biol. Med.* **8,** 541–543 CrossRef Medline
33. Heeringa, S. F., Chernin, G., Chaki, M., Zhou, W., Sloan, A. J., Ji, Z., Xie, L. X., Salviati, L., Hurd, T. W., Vega-Warner, V., Killen, P. D., Raphael, Y., Ashraf, S., Ovunc, B., Schoeb, D. S., *et al.* (2011) COQ6 mutations in human patients produce nephrotic syndrome with sensorineural deafness. *J. Clin. Invest.* **121,** 2013–2024 CrossRef Medline
34. Nguyen, T. P., Casarin, A., Desbats, M. A., Doimo, M., Trevisson, E., Santos-Ocaña, C., Navas, P., Clarke, C. F., and Salviati, L. (2014) Molecular characterization of the human COQ5 *C*-methyltransferase in coenzyme Q_{10} biosynthesis. *Biochim. Biophys. Acta* **1841,** 1628–1638 CrossRef Medline
35. Conrad, M., Schothorst, J., Kankipati, H. N., Van Zeebroeck, G., Rubio-Texeira, M., and Thevelein, J. M. (2014) Nutrient sensing and signaling in the yeast *Saccharomyces cerevisiae*. *FEMS Microbiol. Rev.* **38,** 254–299 CrossRef Medline
36. Glick, B. S., and Pon, L. A. (1995) Isolation of highly purified mitochondria from *Saccharomyces cerevisiae*. *Methods Enzymol.* **260,** 213–223 CrossRef Medline
37. Stefely, J. A., Reidenbach, A. G., Ulbrich, A., Oruganty, K., Floyd, B. J., Jochem, A., Saunders, J. M., Johnson, I. E., Minogue, C. E., Wrobel, R. L., Barber, G. E., Lee, D., Li, S., Kannan, N., Coon, J. J., *et al.* (2015) Mitochondrial ADCK3 employs an atypical protein kinase-like fold to enable coenzyme Q biosynthesis. *Mol. Cell* **57,** 83–94 CrossRef Medline
38. Xie, L. X., Hsieh, E. J., Watanabe, S., Allan, C. M., Chen, J. Y., Tran, U. C., and Clarke, C. F. (2011) Expression of the human atypical kinase ADCK3 rescues coenzyme Q biosynthesis and phosphorylation of Coq polypeptides in yeast *coq8* mutants. *Biochim. Biophys. Acta* **1811,** 348–360 CrossRef Medline
39. Xie, L. X., Ozeir, M., Tang, J. Y., Chen, J. Y., Jaquinod, S. K., Fontecave, M., Clarke, C. F., and Pierrel, F. (2012) Overexpression of the Coq8 kinase in *Saccharomyces cerevisiae coq* null mutants allows for accumulation of diagnostic intermediates of the coenzyme Q_6 biosynthetic pathway. *J. Biol. Chem.* **287,** 23571–23581 CrossRef Medline
40. Tran, U. C., and Clarke, C. F. (2007) Endogenous synthesis of coenzyme Q in eukaryotes. *Mitochondrion* **7,** Suppl., S62–S71 CrossRef Medline
41. Wang, Y., and Hekimi, S. (2019) The complexity of making ubiquinone. *Trends Endocrinol. Metab.* **30,** 929–943 CrossRef Medline
42. Murley, A., and Nunnari, J. (2016) The emerging network of mitochondria-organelle contacts. *Mol. Cell* **61,** 648–653 CrossRef Medline
43. Kehrein, K., Möller-Hergt, B. V., and Ott, M. (2015) The MIOREX complex–lean management of mitochondrial gene expression. *Oncotarget* **6,** 16806–16807 CrossRef Medline
44. Fontanesi, F. (2013) Mechanisms of mitochondrial translational regulation. *IUBMB Life* **65,** 397–408 CrossRef Medline
45. Marchler-Bauer, A., Zheng, C., Chitsaz, F., Derbyshire, M. K., Geer, L. Y., Geer, R. C., Gonzales, N. R., Gwadz, M., Hurwitz, D. I., Lanczycki, C. J., Lu, F., Lu, S., Marchler, G. H., Song, J. S., Thanki, N., *et al.* (2013) CDD: conserved domains and protein three-dimensional structure. *Nucleic Acids Res.* **41,** D348–D352 CrossRef Medline
46. Rossmann, M. G., Moras, D., and Olsen, K. W. (1974) Chemical and biological evolution of nucleotide-binding protein. *Nature* **250,** 194–199 CrossRef Medline
47. Kopec, J., Schnell, R., and Schneider, G. (2011) Structure of PA4019, a putative aromatic acid decarboxylase from *Pseudomonas aeruginosa*. *Acta Crystallogr. Sect. F Struct. Biol. Cryst. Commun.* **67,** 1184–1188 CrossRef Medline
48. Guarás, A., Perales-Clemente, E., Calvo, E., Acín-Pérez, R., Loureiro-Lopez, M., Pujol, C., Martínez-Carrascoso, I., Nuñez, E., García-Marqués, F., Rodríguez-Hernández, M. A., Cortés, A., Diaz, F., Pérez-Martos, A., Moraes, C. T., Fernández-Silva, P., *et al.* (2016) The $CoQH_2$/CoQ ratio serves as a sensor of respiratory chain efficiency. *Cell Rep.* **15,** 197–209 CrossRef Medline
49. Scialò, F., Sriram, A., Fernández-Ayala, D., Gubina, N., Lõhmus, M., Nelson, G., Logan, A., Cooper, H. M., Navas, P., Enríquez, J. A., Murphy, M. P., and Sanz, A. (2016) Mitochondrial ROS produced via reverse electron transport extend animal lifespan. *Cell Metab.* **23,** 725–734 CrossRef Medline
50. UniProt Consortium (2018) UniProt: the universal protein knowledgebase. *Nucleic Acids Res.* **46,** 2699 CrossRef Medline
51. Pagliarini, D. J., Calvo, S. E., Chang, B., Sheth, S. A., Vafai, S. B., Ong, S. E., Walford, G. A., Sugiana, C., Boneh, A., Chen, W. K., Hill, D. E., Vidal, M., Evans, J. G., Thorburn, D. R., Carr, S. A., and Mootha, V. K. (2008) A mitochondrial protein compendium elucidates complex I disease biology. *Cell* **134,** 112–123 CrossRef Medline
52. van den Bosch, B. J., Gerards, M., Sluiter, W., Stegmann, A. P., Jongen, E. L., Hellebrekers, D. M., Oegema, R., Lambrichs, E. H., Prokisch, H., Danhauser, K., Schoonderwoerd, K., de Coo, I. F., and Smeets, H. J. (2012) Defective NDUFA9 as a novel cause of neonatally fatal complex I disease. *J. Med. Genet.* **49,** 10–15 CrossRef Medline
53. Brachmann, C. B., Davies, A., Cost, G. J., Caputo, E., Li, J., Hieter, P., and Boeke, J. D. (1998) Designer deletion strains derived from *Saccharomyces cerevisiae* S288C: a useful set of strains and plasmids for PCR-mediated gene disruption and other applications. *Yeast* **14,** 115–132 CrossRef Medline
54. Thomas, B. J., and Rothstein, R. (1989) Elevated recombination rates in transcriptionally active DNA. *Cell* **56,** 619–630 CrossRef Medline
55. Barkovich, R. J., Shtanko, A., Shepherd, J. A., Lee, P. T., Myles, D. C., Tzagoloff, A., and Clarke, C. F. (1997) Characterization of the *COQ5* gene from *Saccharomyces cerevisiae.* Evidence for a *C*-methyltransferase in ubiquinone biosynthesis. *J. Biol. Chem.* **272,** 9182–9188 CrossRef Medline

56. Rothstein, R. J. (1983) One-step gene disruption in yeast. *Methods Enzymol.* **101,** 202–211 CrossRef Medline
57. Gietz, R. D., and Woods, R. A. (2002) Transformation of yeast by lithium acetate/single-stranded carrier DNA/polyethylene glycol method. *Methods Enzymol.* **350,** 87–96 CrossRef Medline
58. Hill, S., Hirano, K., Shmanai, V. V., Marbois, B. N., Vidovic, D., Bekish, A. V., Kay, B., Tse, V., Fine, J., Clarke, C. F., and Shchepinov, M. S. (2011) Isotope-reinforced polyunsaturated fatty acids protect yeast cells from oxidative stress. *Free Radic. Biol. Med.* **50,** 130–138 CrossRef Medline
59. Hill, S., Lamberson, C. R., Xu, L., To, R., Tsui, H. S., Shmanai, V. V., Bekish, A. V., Awad, A. M., Marbois, B. N., Cantor, C. R., Porter, N. A., Clarke, C. F., and Shchepinov, M. S. (2012) Small amounts of isotope-reinforced polyunsaturated fatty acids suppress lipid autoxidation. *Free Radic. Biol. Med.* **53,** 893–906 CrossRef Medline
60. Santos, J. H., Mandavilli, B. S., and Van Houten, B. (2002) Measuring oxidative mtDNA damage and repair using quantitative PCR. *Methods Mol. Biol.* **197,** 159–176 CrossRef Medline
61. Gonzalez-Hunt, C. P., Rooney, J. P., Ryde, I. T., Anbalagan, C., Joglekar, R., and Meyer, J. N. (2016) PCR-based analysis of mitochondrial DNA copy number, mitochondrial DNA damage, and nuclear DNA damage. *Curr. Protoc. Toxicol.* **67,** 20.11.1–20.11.25 CrossRef Medline
62. Guo, X., Niemi, N. M., Hutchins, P. D., Condon, S. G. F., Jochem, A., Ulbrich, A., Higbee, A. J., Russell, J. D., Senes, A., Coon, J. J., and Pagliarini, D. J. (2017) Ptc7p dephosphorylates select mitochondrial proteins to enhance metabolic function. *Cell Rep.* **18,** 307–313 CrossRef Medline
63. Eyer, P., Worek, F., Kiderlen, D., Sinko, G., Stuglin, A., Simeon-Rudolf, V., and Reiner, E. (2003) Molar absorption coefficients for the reduced Ellman reagent: reassessment. *Anal. Biochem.* **312,** 224–227 CrossRef Medline
64. Zhang, T., Lei, J., Yang, H., Xu, K., Wang, R., and Zhang, Z. (2011) An improved method for whole protein extraction from yeast *Saccharomyces cerevisiae*. *Yeast* **28,** 795–798 CrossRef Medline
65. Schägger, H., Cramer, W. A., and von Jagow, G. (1994) Analysis of molecular masses and oligomeric states of protein complexes by blue native electrophoresis and isolation of membrane protein complexes by two-dimensional native electrophoresis. *Anal. Biochem.* **217,** 220–230 CrossRef Medline
66. Wittig, I., Braun, H. P., and Schägger, H. (2006) Blue NativePAGE. *Nat. Protoc.* **1,** 418–428 CrossRef Medline
67. Barros, M. H., and Tzagoloff, A. (2017) Aep3p-dependent translation of yeast mitochondrial *ATP8*. *Mol. Biol. Cell* **28,** 1426–1434 CrossRef Medline
68. Santos-Ocaña, C., Do, T. Q., Padilla, S., Navas, P., and Clarke, C. F. (2002) Uptake of exogenous coenzyme Q and transport to mitochondria is required for bc_1 complex stability in yeast *coq* mutants. *J. Biol. Chem.* **277,** 10973–10981 CrossRef Medline
69. Winzeler, E. A., Shoemaker, D. D., Astromoff, A., Liang, H., Anderson, K., Andre, B., Bangham, R., Benito, R., Boeke, J. D., Bussey, H., Chu, A. M., Connelly, C., Davis, K., Dietrich, F., Dow, S. W., *et al.* (1999) Functional characterization of the *S. cerevisiae* genome by gene deletion and parallel analysis. *Science* **285,** 901–906 CrossRef Medline
70. Sikorski, R. S., and Hieter, P. (1989) A system of shuttle vectors and yeast host strains designed for efficient manipulation of DNA in *Saccharomyces cerevisiae*. *Genetics* **122,** 19–27 Medline
71. Christianson, T. W., Sikorski, R. S., Dante, M., Shero, J. H., and Hieter, P. (1992) Multifunctional yeast high-copy-number shuttle vectors. *Gene* **110,** 119–122 CrossRef Medline